Argonne NATIONAL LABORATORY

ANL-08/27

Neutronics, Steady-State, and Transient Analyses for the Poland MARIA Reactor for Irradiation Testing of LEU Lead Test Fuel Assemblies from CERCA: ANL Independent Verification Results

Nuclear Engineering Division

About Argonne National Laboratory

Argonne is a U.S. Department of Energy laboratory managed by UChicago Argonne, LLC under contract DE-AC02-06CH11357. The Laboratory's main facility is outside Chicago, at 9700 South Cass Avenue, Argonne, Illinois 60439. For information about Argonne and its pioneering science and technology programs, see www.anl.gov.

Availability of This Report

This report is available, at no cost, at http://www.osti.gov/bridge. It is also available on paper to the U.S. Department of Energy and its contractors, for a processing fee, from:

U.S. Department of Energy
Office of Scientific and Technical Information
P.O. Box 62
Oak Ridge, TN 37831-0062
phone (865) 576-8401
fax (865) 576-5728
reports@adonis.osti.gov

Disclaimer

This report was prepared as an account of work sponsored by an agency of the United States Government. Neither the United States Government nor any agency thereof, nor UChicago Argonne, LLC, nor any of their employees or officers, makes any warranty, express or implied, or assumes any legal liability or responsibility for the accuracy, completeness, or usefulness of any information, apparatus, product, or process disclosed, or represents that its use would not infringe privately owned rights. Reference herein to any specific commercial product, process, or service by trade name, trademark, manufacturer, or otherwise, does not necessarily constitute or imply its endorsement, recommendation, or favoring by the United States Government or any agency thereof. The views and opinions of document authors expressed herein do not necessarily state or reflect those of the United States Government or any agency thereof, Argonne National Laboratory, or UChicago Argonne, LLC.

ANL-08/27

Neutronics, Steady-State, and Transient Analyses for the Poland MARIA Reactor for Irradiation Testing of LEU Lead Test Fuel Assemblies from CERCA: ANL Independent Verification Results

by
P.L. Garner and N.A. Hanan
Nuclear Engineering Division, Argonne National Laboratory

August 2008

Neutronics, Steady-State, and Transient Analyses for the Poland MARIA Reactor for Irradiation Testing of LEU Lead Test Fuel Assemblies from CERCA: ANL Independent Verification Results

P.L. Garner and N. A. Hanan

1. Summary

The MARIA reactor at the Institute of Atomic Energy (IAE) in Swierk (30 km SE of Warsaw) in the Republic of Poland is considering conversion from high-enriched uranium (HEU) to low-enriched uranium (LEU) fuel assemblies (FA). The FA design in MARIA is rather unique; a suitable LEU FA has never been designed or tested. IAE has contracted with CERCA (the fuel supply portion of AREVA in France) to supply 2 lead test assemblies (LTA). The LTAs will be irradiated in MARIA to burnup level of at least 40% for both LTAs and to 60% for one LTA. IAE may decide to purchase additional LEU FAs for a full core conversion after the test irradiation.

The Reactor Safety Committee within IAE and the National Atomic Energy Agency in Poland (PAA) must approve the LTA irradiation process. The approval will be based, in part, on IAE submitting revisions to portions of the Safety Analysis Report (SAR) which are affected by the insertion of the LTAs. (A similar process will be required for the full core conversion to LEU fuel.) The analysis required was established during working meetings between Argonne National Laboratory (ANL) and IAE staff during August 2006, subsequent email correspondence, and subsequent staff visits. The analysis needs to consider the current high-enriched uranium (HEU) core and 4 core configurations containing 1 and 2 LEU LTAs in various core positions.

Calculations have been performed at ANL in support of the LTA irradiation. These calculations are summarized in this report and include criticality, burn-up, neutronics parameters, steady-state thermal hydraulics, and postulated transients. These calculations have been performed at the request of the IAE staff, who are performing similar calculations to be used in their SAR amendment submittal to the PAA. The ANL analysis has been performed independently from that being performed by IAE and should only be used as one step in the verification process.

2. Reactor Information

2.1. General

The multipurpose high flux research reactor MARIA is a water and beryllium moderated reactor of a pool type with graphite reflector and pressurized channels containing concentric six-tube assemblies of fuel elements. A vertical cross-section of the reactor pool is shown in Figure 2.1.1. The fuel channels are situated in a matrix (cf. Fig. 2.1.2) containing beryllium blocks and enclosed by lateral reflector made of graphite blocks in aluminum cans. Each fuel channel has a separate valved connection to the inlet and outlet headers for forced flow of coolant. There is a

separate cooling loop for the reactor pool. The MARIA reactor is equipped with vertical channels for irradiation of target materials, a rabbit system and six horizontal neutron beam channels. The MARIA reactor reached its first criticality in December 1974. Typical activities in MARIA are materials irradiation, neutron scattering, neutron radiography, and neutron modification of materials. [Extracted from Ref. 1.]

2.2. HEU

The reactor is currently fueled with MR-6-430 type fuel assemblies (FA). The fuel material is UO_2-Al clad in Al with 36% enrichment in U-235; there are 430 g of U-235 per FA. The fuel is contained in the central 1 m length of 6 concentric circular tubes as shown in Fig 2.2.1. The tube numbering convention is from inner (=1) to outer (=6) in this report. The coolant gap between tubes is 2.5 mm. Coolant flow is downward outside of tube 4, turns below the fuel tubes, and is upward inside of tube 4. A non-fueled extension above tube 4 separates down- from up-flow. [Extracted from Ref. 2.] Nominal coolant flow rate is 25 m^3/h per FA.

2.3. LEU LTA

The LEU LTAs from CERCA are similar to the current HEU FA with the following notable exceptions. Fuel enrichment will be 20% in U-235; there are 485 g of U-235 per FA. Tube 1 will have no fuel. The fuel meat is U_3Si_2 and is 0.8 mm thick; the cladding is 0.6 mm thick. Each fuel tube consists of 3 azimuthal segments of somewhat less than 120 degrees each. The segments are joined together using an aluminum spacer (bigger than the rib in the HEU design) which also helps maintain tube-to-tube separation. Nominal coolant flow rate is expected to be 26 m^3/h per FA. [Extracted from Ref. 3. More exact details of the FA design are considered proprietary by CERCA.]

2.4. Neutronics

Five core configurations are expected during the LTA irradiation: (1) full HEU core, (2) LTA-1 in core position i-5 (low power) for 1 week, (3) LTA-1 moved to core position h-7 (high power) for 1 week, (4) LTA-2 in core position i-5 for 1 week and LTA-1 continues in core position h-7, and (5) LTA-2 moved to core position h-6 (high power) and LTA-1 continues in core position h-7. Operation in configuration 5 continues until 40% burnup in the LTAs is achieved; this is expected to take approximately 1 year; one LTA will be removed at that time for inspection. Irradiation of the other LTA is anticipated to continue to 60% burnup. Calculations start with the HEU core condition on 31 March 2008. All cores contain 24 FAs. Reactor power is assumed to be 16 MW during the irradiation.

The MCNP code [Ref. 4] was used to calculate the shutdown margin, individual worth of control rods, detailed power distribution, and various other neutronics parameters for the 5 cores. The MC-REBUS code [Ref. 5] was used for the burnup calculations.

Figure 2.4.1 demonstrates good agreement between burnup calculated using MC-REBUS and operational data for the first 4 days of the Mar/31/08 core HEU core operation cycle. Figure 2.4.2 shows the burnup calculated for the first week of each of the 5 core configurations.

The power vs. time history for each of these cycles is exactly the same as normally used for the current HEU core.

Kinetics parameters are shown in Table 2.4.1 for beginning of cycle (BOC) and in Table 2.4.2 for end of cycle (EOC) for each of the 5 core configurations. There is little change in any of these parameters across the 5 core configurations. The feedback coefficients at EOC will be used in all transient analyses since these values are somewhat less negative than the values at BOC and that is a conservative choice.

Reactivity worths of the individual control rods (denoted "PK") and the regulating power automatic rod (denoted PAR) are shown in Table 2.4.3 for the 5 core configurations. The combined worth of the 6 safety rods (denoted "PB") is shown in the first row of Table 2.4.4; the combined worth of all but the highest-worth safety rod is shown in row 2. The electromagnetic latch of all rods is identical and all are connected to the scram logic; therefore, scram reactivity is based on motion of all rods but assuming the highest worth rod is stuck; these total worths are shown in row 3 of Table 2.4.4 and are the values used in the transient calculations. Control rod worth is a function of position having the usual "S" shape, as shown in Figures 2.4.3, 2.4.4, and 2.4.5 on a relative basis for the control, safety, and regulating rods, respectively. Figure 2.4.6 shows the control rod position versus time after scram as measured in MARIA. The combination of these pieces (i.e., total worth, worth vs. position, and position vs. time) are used to construct worth vs. time after scram for use in the transient calculations. There is a 0.2 s delay between crossing any power limit setpoint and start of control rod motion for scram. The shutdown margin for all 5 core configurations is shown in Table 2.4.5; this criterion is defined as the reactivity with all control and regulating rods fully inserted and all safety rods fully withdrawn.

1. collector of the fuel channels cooling circuit
2. control rods drives truck
3. collector of the reactor pool cooling circuit
4. cutting-off machine at water sluice
5. water sluice bulkheads
6. shielding box
7. ventilation duct of the storage pool
8. shifter
9. dismantling cell
10. crane Q = 3.5 T
11. collector of the reactor pool cooling circuit
12. sink basin
13. tube for fuel channel dismantling
14. ventilation channel
15. installation duct
16. baffle
17. reactor pool
18. storage pool
19. stationary bulkhead

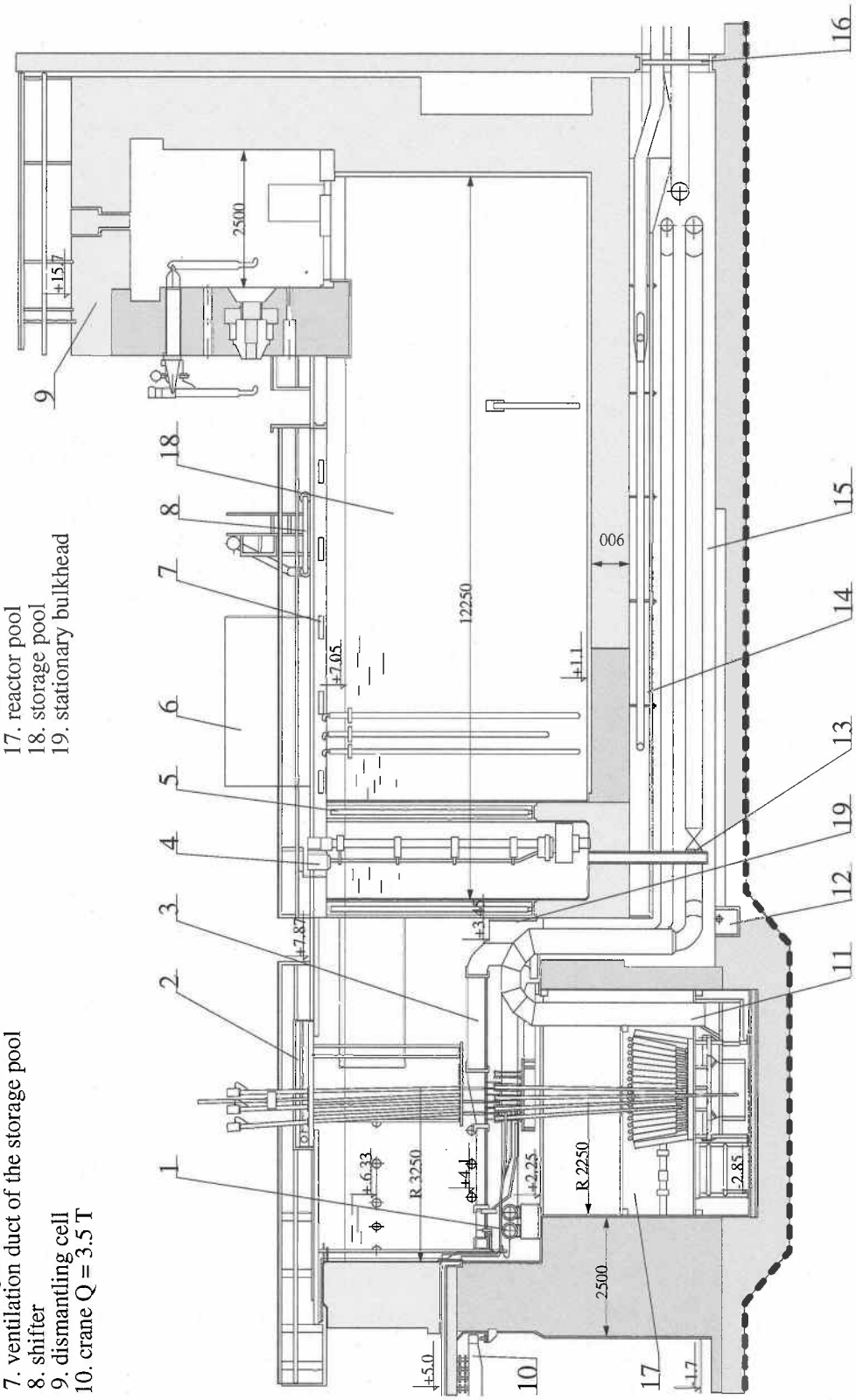

Figure 2.1.1 Elevation View of Reactor

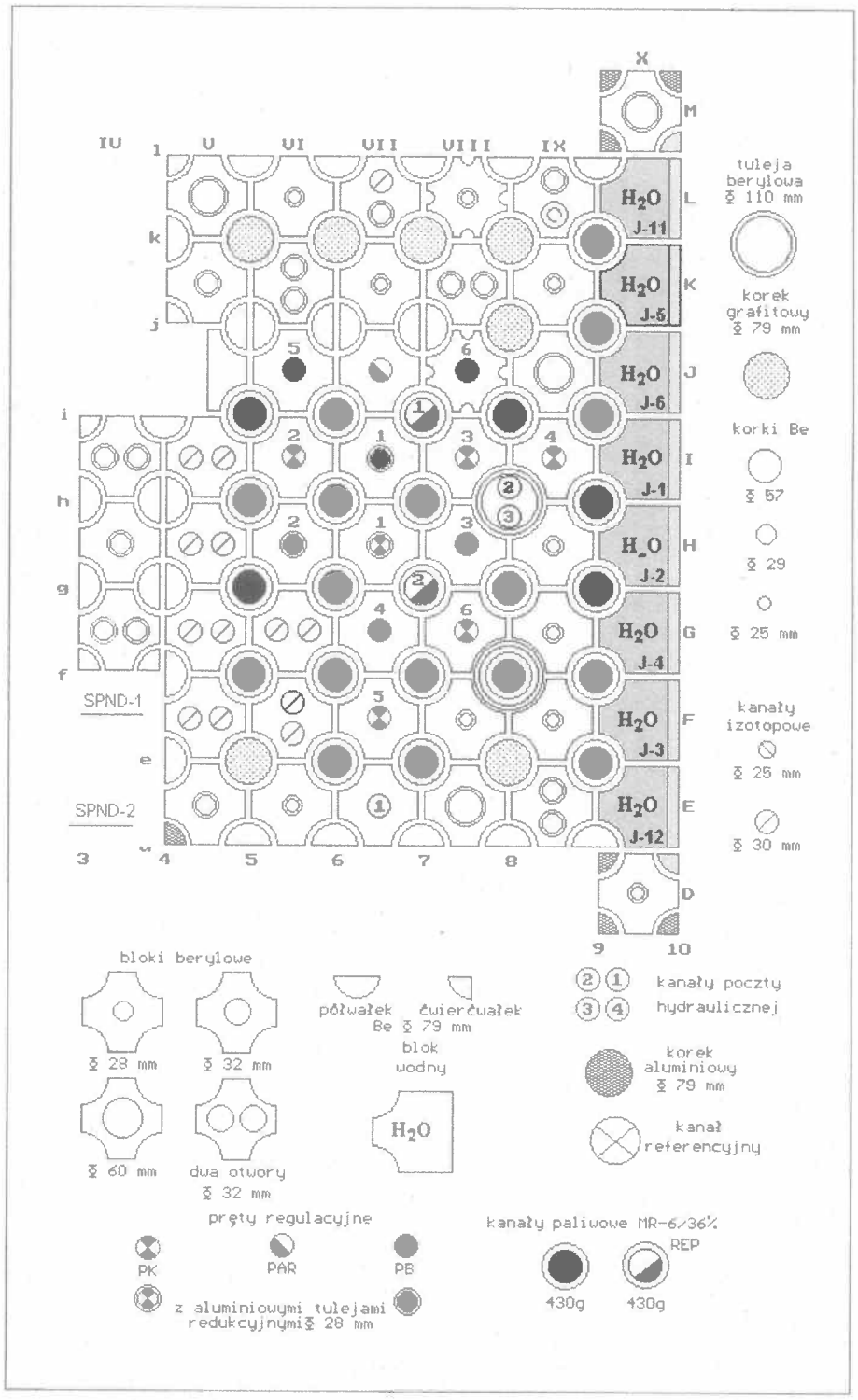

REACTOR MARIA
Core configuration
(KKR - 01/2008)

Figure 2.1.2 Reactor Configuration on 31 March 2008 (Note: Bottom of figure shows legend for the 3 control rod types and the fuel assemblies.)

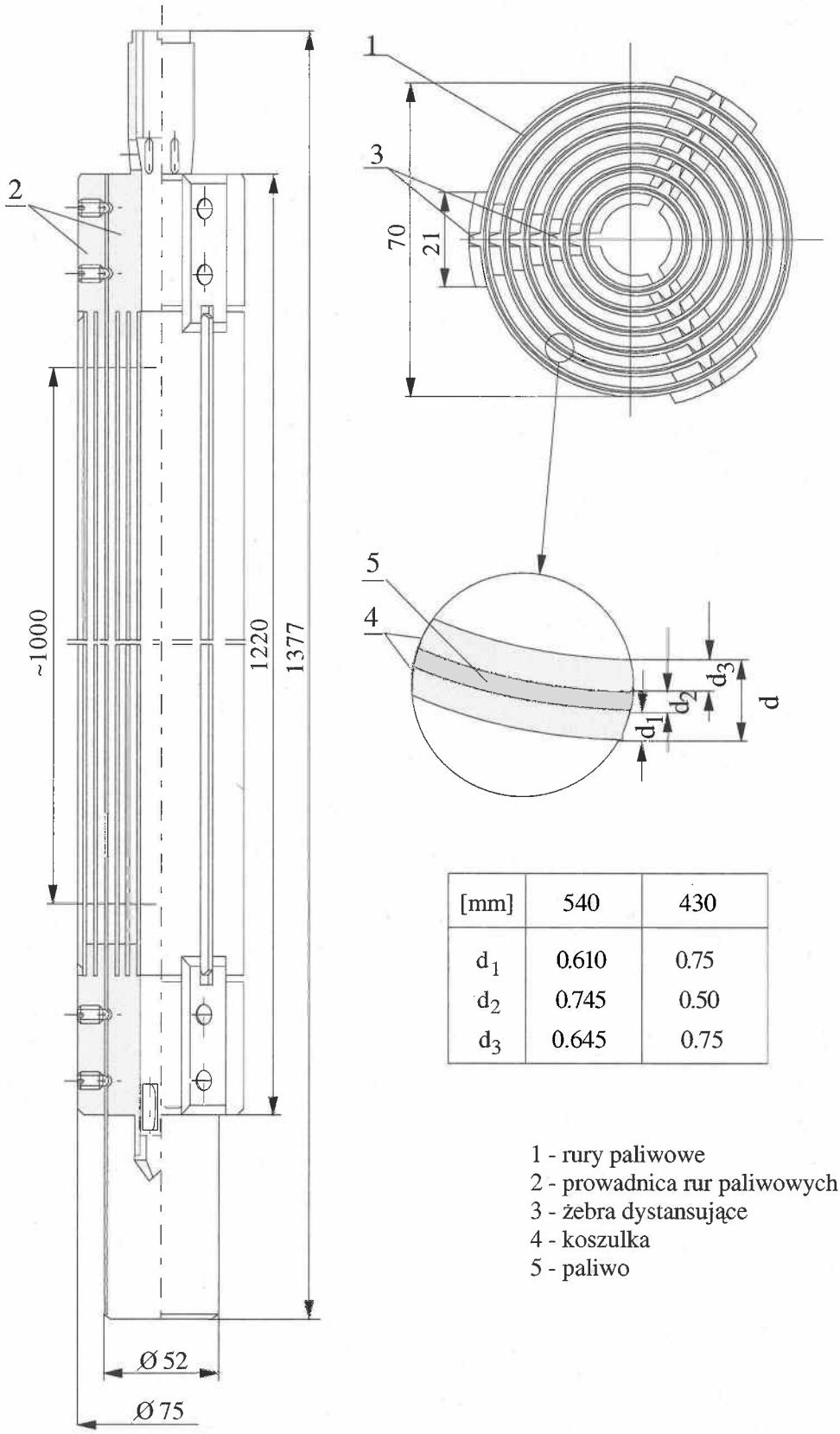

[mm]	540	430
d_1	0.610	0.75
d_2	0.745	0.50
d_3	0.645	0.75

1 - rury paliwowe
2 - prowadnica rur paliwowych
3 - żebra dystansujące
4 - koszulka
5 - paliwo

Figure 2.2.1 HEU Fuel Assembly (Legend: 1: fuel tubes, 2: fuel tubes guide bar, 3: spacer ribs, 4: clad, 5: fuel. The bottom of the FA is at the top of the figure.)

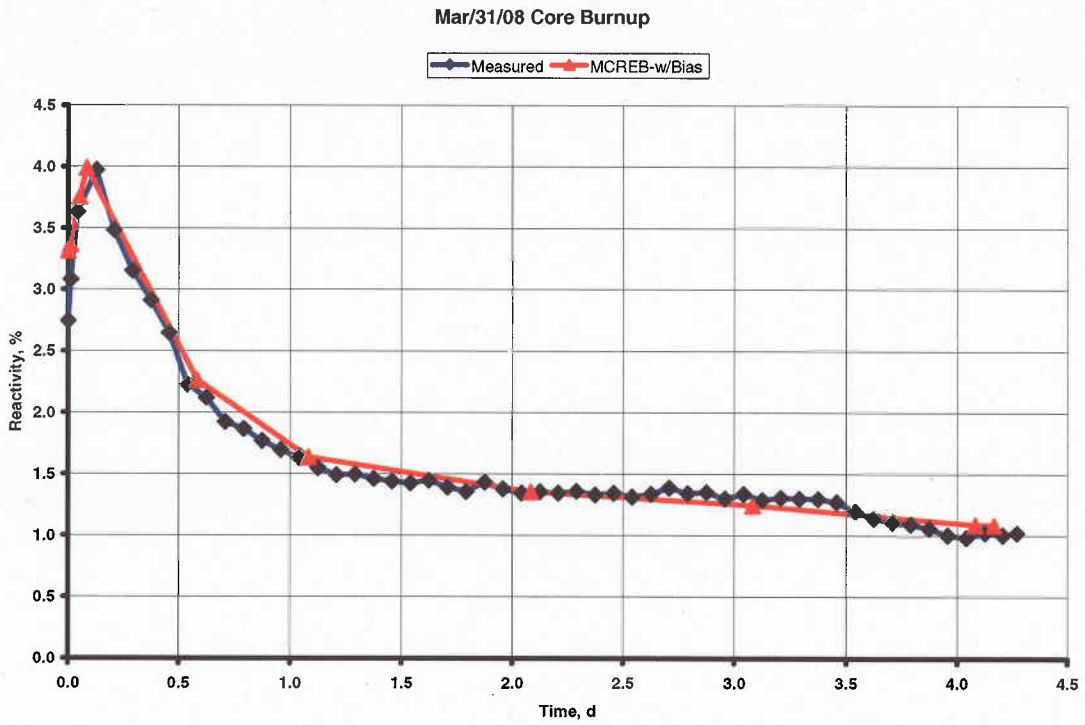

Figure 2.4.1 Comparison between Measured and Calculated Burnup

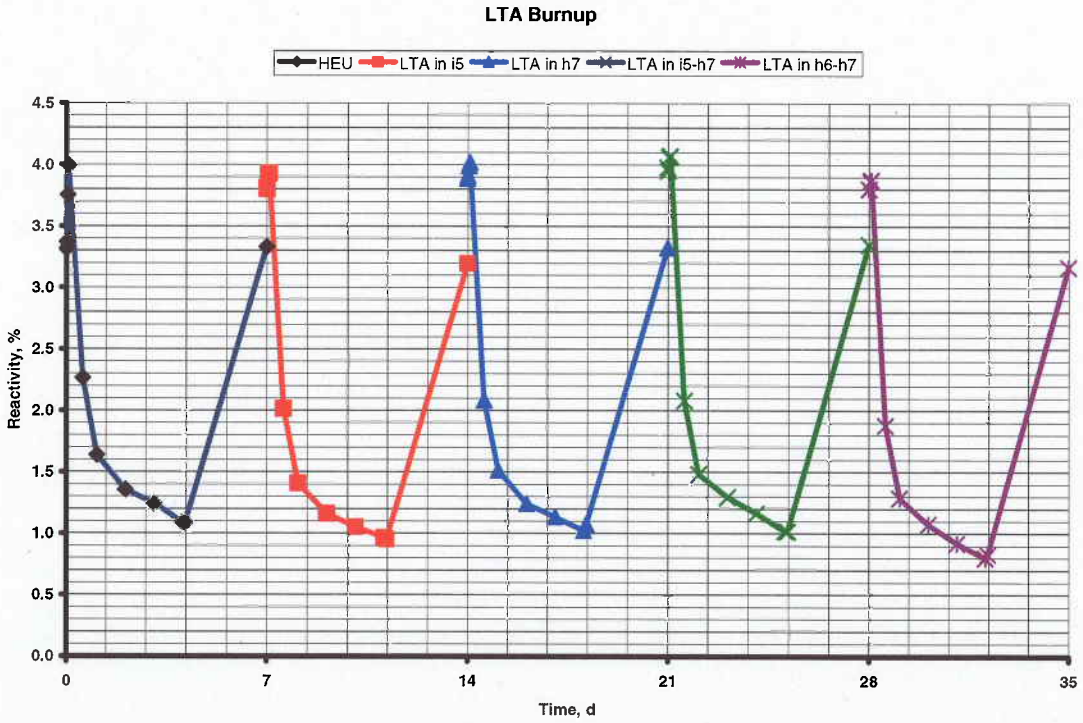

Figure 2.4.2 Burnup Calculated for 1 Week of Each Core Configuration

Table 2.4.1 Kinetics Parameters at BOC

LTA BU	HEU	LTA in i-5	LTA in h-7	LTA in i-5 & h-7	LTA in h-6 & h-7	LTA in h-6 & h-7 20%	LTA in h-6 & h-7 40%	LTA in h-6 & h-7 60%
Temperature Coefficient – FA - (¢/°C):								
294 - 400 C	-2.4	-2.4	-2.3	-2.4	-2.3	-2.4	-2.6	-2.8
400 - 600 C	-2.2	-2.2	-2.1	-2.1	-2.1	-2.2	-2.4	-2.5
294 - 600 C	-2.3	-2.3	-2.2	-2.2	-2.2	-2.3	-2.5	-2.6
Void Coefficient – FA - (¢/%void):								
0 - 5%	-8.1	-6.8	-6.6	-7.3	-7.3	-7.4	-7.0	-6.5
5 - 10 %	-8.4	-7.8	-8.5	-8.1	-8.1	-7.7	-7.8	-8.0
0 - 10 %	-8.2	-7.3	-7.6	-7.7	-7.7	-7.5	-7.4	-7.2
Doppler Coefficient (¢/°C):								
294 - 400 K	-0.1	-0.1	-0.1	-0.1	-0.1	-0.1		
400 - 600 K	-0.1	-0.1	-0.1	-0.1	-0.1	-0.1		
294 - 600 K	-0.1	-0.1	-0.1	-0.1	-0.1	-0.1		
Be Reflector (¢/°C):								
294 - 400 C	1.4	1.4	1.4	1.4	1.3			
Temperature Coefficient – H2O Reflector – (¢/°C):								
294 - 400 C	1.4	1.4	1.4	1.4	1.4			
Void Coefficient – Reflector – (¢/%void):								
0 - 5%	5.1	5.4	5.0	5.0	4.9			
Delayed Neutron Fraction (x 1.0e+3):	698.5	697.3	696.1	696.1	696.9	694.7	692.6	692.4
Generation Time, μs:	153.4	157.4	152.4	154.3	152.5	158.5	166.4	172.4

Table 2.4.2 Kinetics Parameters at EOC

	HEU	LTA in i-5	LTA in h-7	LTA in i-5 & h-7	LTA in h-6 & h-7
Temperature Coefficient - FA - (¢/°C):					
294 - 400 C	-2.3	-2.3	-2.2	-2.2	-2.2
400.- 600 C	-2.0	-2.0	-1.9	-1.9	-1.9
294 - 600 C	-2.1	-2.1	-2.0	-2.0	-2.0
Void Coefficient - FA - (¢/%void):					
0 - 5%	-6.2	-5.8	-5.6	-5.8	-5.7
5 - 10 %	-6.4	-6.0	-6.7	-6.4	-6.5
0 - 10 %	-6.3	-5.9	-6.2	-6.1	-6.1
Doppler Coefficient (¢/°C):					
294 - 400 K	-0.1	-0.1	-0.1	-0.1	-0.1
400 - 600 K	-0.1	-0.1	-0.1	-0.1	-0.1
294 - 600 K	-0.1	-0.1	-0.1	-0.1	-0.1
Delayed Neutron Fraction (x 1.0e+3):	696.0	697.3	695.9	696.0	696.8
Generation Time, μs:	158.7	160.5	159.1	158.8	158.5

Table 2.4.3 Reactivity Worth [$] of Control Rods (PK)

	HEU MAR/31/08	LTA in i-5	LTA in h-7	LTA in i-5 & h-7	LTA in h-6 & h-7
PK-1	4.11	4.02	4.37	4.29	4.41
PK-2	2.34	2.43	2.19	2.51	2.48
PK-3	1.02	0.97	1.17	1.2	1.22
PK-4	0.18	0.15	0.23	0.23	0.22
PK-5	1.42	1.52	1.45	1.44	1.41
PK-6	1.5	1.57	1.64	1.58	1.56
PAR	0.68	0.62	0.63	0.69	0.69

Table 2.4.4 SCRAM Reactivity [$]

	Stuck PB	HEU MAR/31/08	LTA in i-5	LTA in h-7	LTA in i-5 & h-7	LTA in h-6 & h-7
Safety Only	No	12.67	12.44	12.78	12.91	13.07
Safety Only	Yes	7.96	8.14	8.45	8.62	8.68
All Rods	Yes	15.14	14.8	15.73	15.13	15.31

Table 2.4.5 Shutdown Margin [$]

	HEU MAR/31/08	LTA in i-5	LTA in h-7	LTA in i-5 and h-7	LTA in h-6 and h-7
	-6.78	-5.87	-6.14	-6.18	-6.51

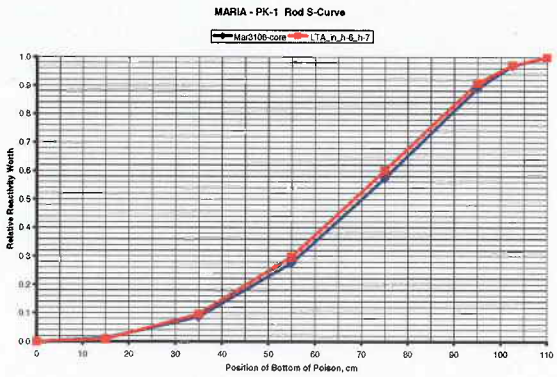

Figure 2.4.3 Control Rod Worth vs. Position

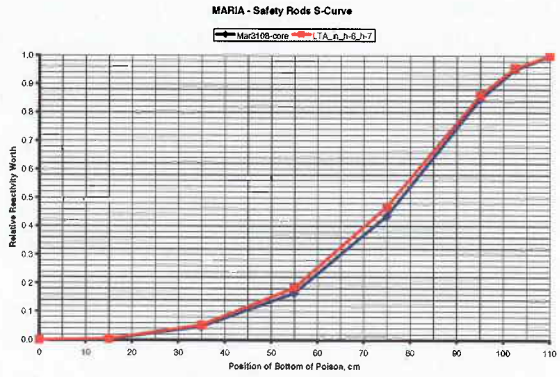

Figure 2.4.4 Safety Rod Worth vs. Position

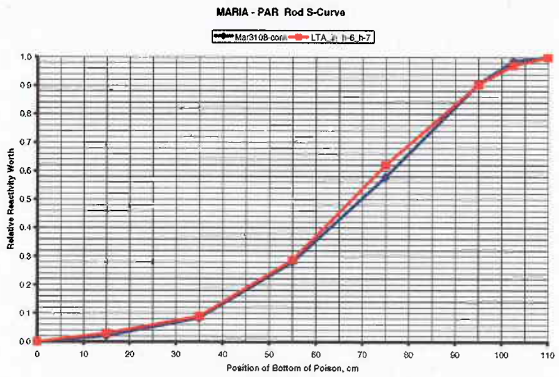

Figure 2.4.5 Regulating Rod Worth vs. Position

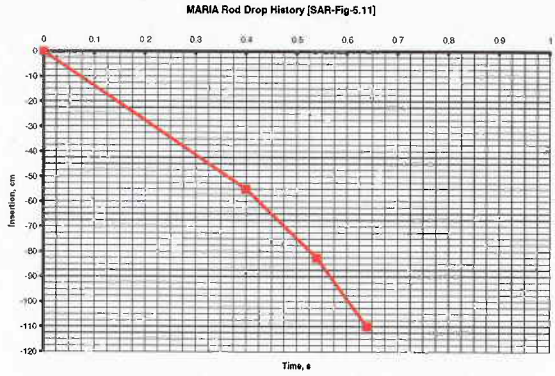

Figure 2.4.6 Rod Position vs. Time After Scram

3. Steady-State Analysis

3.1. Model

Steady-state (and transient) thermalhydraulic analyses were performed using the RELAP5 code [Ref. 6]. The noding diagram for the HEU core is shown in Figure 3.1.1.

The noding for a single HEU FA will be described using the component numbers in the left portion of Figure 3.1.1. The fuel element tubes 1 through 6 are represented by heat structures 2801, 2701, 2201, 1801, 1701, and 1201, respectively; the 1 m fueled length is divided into 20 axial nodes. The central unheated tube 0 is represented by heat structure 2901. Coolant flows downward toward the fuel tubes using pipe-type component 115. The coolant splits and continues downward adjacent to tubes 4 (outside), 5, and 6 using pipe components 180, 170, and 120, respectively. At the bottom of the fuel, the flow continues downward, turns inward, and flows upward using branches 190, 194, and 200. The flow continues upward adjacent to tubes 0 through 4 (inside) using pipe components 210, 290, 280, 270, and 220, respectively. The flow streams rejoin and continue upward flow using pipe component 295. Heat structure 1151 allows for energy transfer between the inlet and outlet components. There is no azimuthal variation within any of these components.

Noding for a single LEU FA is similar to the HEU FA noding except tube 0 is deleted and tube 1 has no fuel. All flow areas, hydraulic diameters, fuel and clad thickness, and fuel tube azimuthal extent are different between the HEU and LEU models.

This set of components is replicated for each grouping of FA to be represented. For the HEU core, one set of components like this represents the FA having the peak power density (e.g., components 315 through 495 in Figure 3.1.1); a second set of components represents in average the other 23 FA in the core (e.g., components 115 through 295 in Figure 3.1.1). For the core with one LTA, one set of components like this represents the LTA, a second set of components represents the HEU FA having the peak power density, and a third set of components represents the other 22 HEU FA in the core. For the core with 2 LTAs, one set of components like this represents LTA-1, a second set of components represents LTA-2, a third set of components represents the HEU FA with the peak power density, and a fourth set of components represents the other 21 HEU FA in the core.

Volume 100 is the core inlet plenum; the core inlet temperature is specified here. Junction 105 specifies the coolant flow rate for the total core. Branch 110 allows the total core flow to be spread across multiple FAs, and branch 980 recollects the outlet flow from all FAs. Volume 900 is the core outlet plenum; the pressure specified here is the reference for other pressures in the calculation.

The MCNP neutronics calculations divide each FA into 21 azimuthal sectors. Each sector is either 12 (near ribs) or 24 (away from ribs) degrees. For each FA type, the sector having the peak power density is identified at the end of the MCNP calculation; the axial distribution of power densities in this sector for all 6 (HEU) or 5 (LEU) tubes is used in a complete 360 degree

model of the FA in RELAP5; this gives the best approximation for calculating peak fuel temperature, even though this results in the total power in this "hot" FA being too high. This is done for the HEU FA having the peak power density, for LTA-1, and for LTA-2. The power density in the portion of the RELAP5 model representing the average HEU FA is then adjusted downward so that the total core power is correct. An assessment of hot channel approximation is presented in Section 3.2

Table 3.1.1 shows the peak power density by fuel type for the 5 cores. The peak power density in the HEU FA is 6.6 GW/m^3 in the all HEU core and decreases to 6.1 GW/m^3 for the cores having LTAs. The peak power density in the LTA is 2.7-2.8 GW/m^3 in position i-5, 4.9 GW/m^3 in position h-7, and 5.2 GW/m^3 in position h-6. Representative radial and axial distributions of power density are shown in Figure 3.1.2 for the peak FA in the all HEU core, in Figure 3.1.3 for LTA-1 in the HEU+LTA-i5 core, and in Figure 3.1.4 for LTA-2 in the HEU+LTA-h6-h7 core. The power density is always highest in the outermost tube of each FA type; this is due to the presence of the beryllium around each FA channel. The power density distribution is lower at the top of the core than at the bottom of the core due to the presence of control rods in the top portion of the core; the axial location of the peak is between 30 and 45% of core height.

Figure 3.1.5 show the power density distribution as a function of azimuthal position at the axial location of peak power density in the FA having the peak power density in the HEU core. The ribs in the HEU FA (and the spacers in the LEU FA) are present at 0 (and 360), 120, and 240 degrees. The power density varies by ±3% around the circumference. The peak occurs mid-way between ribs. Similar information is shown in Figure 3.1.6 for the HEU+LTA-h6-h7 core. The power density in the peak HEU FA varies by ±3% around the circumference; the peak occurs mid-way between ribs. The power density in the peak LEU FA varies by ±17% around the circumference, which is much larger than in the HEU part of the core; the peak occurs adjacent to the spacer and is caused in part by the lack of fuel continuity in the azimuthal direction.

Boundary conditions for the steady-state calculations are as follows. Inlet temperature is 323 K (50°C). Nominal coolant flow rate is 25 m^3/h per HEU FA and 26 m^3/h per LEU FA; this means the total core coolant flow rate (which is the input quantity) is different for the HEU, HEU plus 1 LTA, and HEU plus 2 LTA cores. The flow rate used in the steady-state calculations is 90% of the nominal value just stated. The outlet pressure is 1.4 MPa. For the calculations reported here, heat transfer through the channel wall to the pool is neglected; although this may amount to 5 to 10% of the heat generation, this loss has very little impact on the peak cladding temperature at steady state.

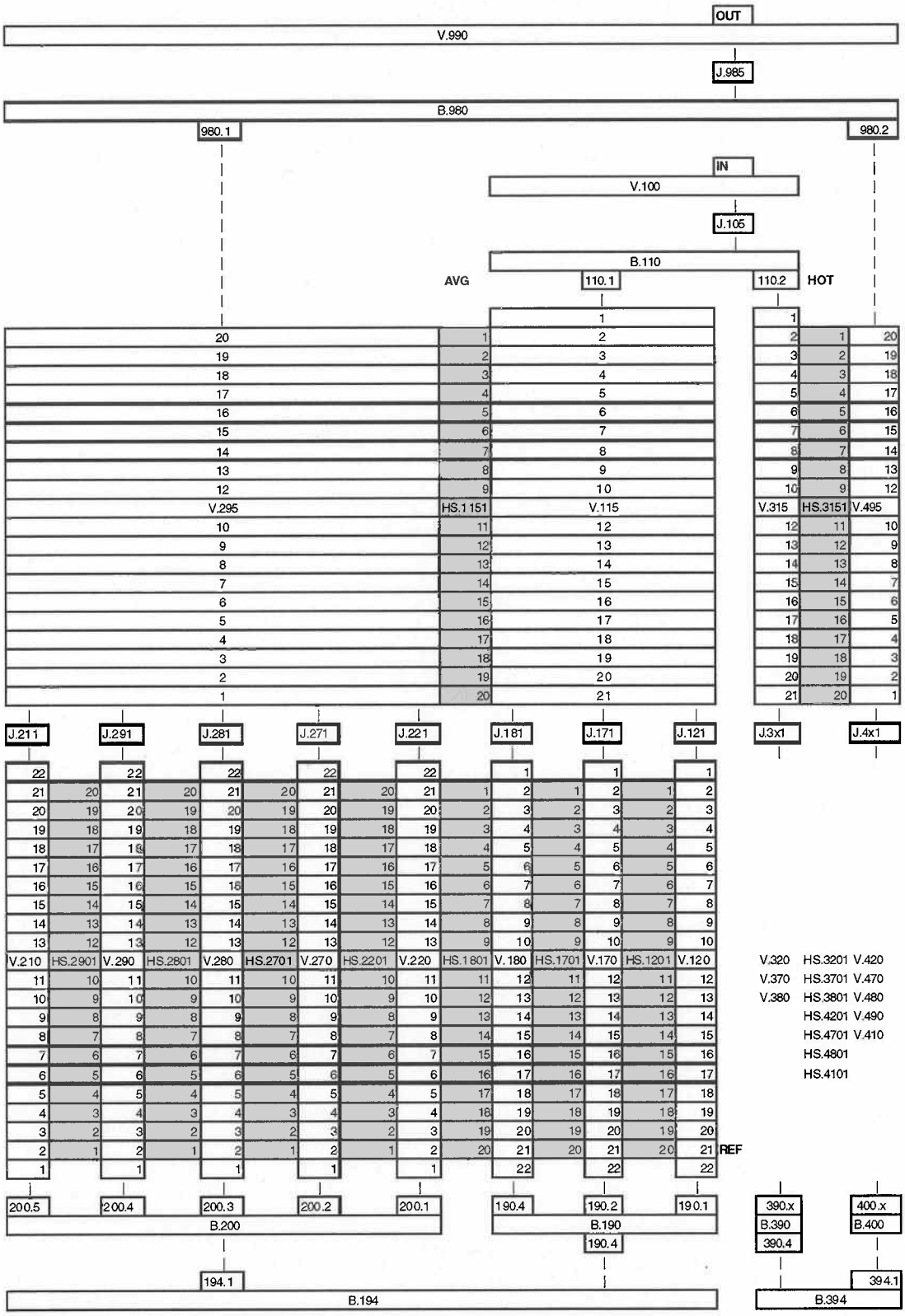

Figure 3.1.1 RELAP5 Noding for HEU Core

Table 3.1.1 Peak Fuel Power Density [GW/m^3]

	HEU MAR/31/08	LTA-1 in i-5	LTA-1 in h-7	LTA-1 in i-5 LTA-2 in h-7	LTA-1 in h-6 LTA-2 in h-7
HEU-avg	2.482	2.325	2.221	2.238	2.096
HEU-peak	6.600	6.106	6.083	6.105	6.107
LTA-1	---	2.741	4.875	4.880	4.873
LTA-2	---	---	---	2.779	5.237

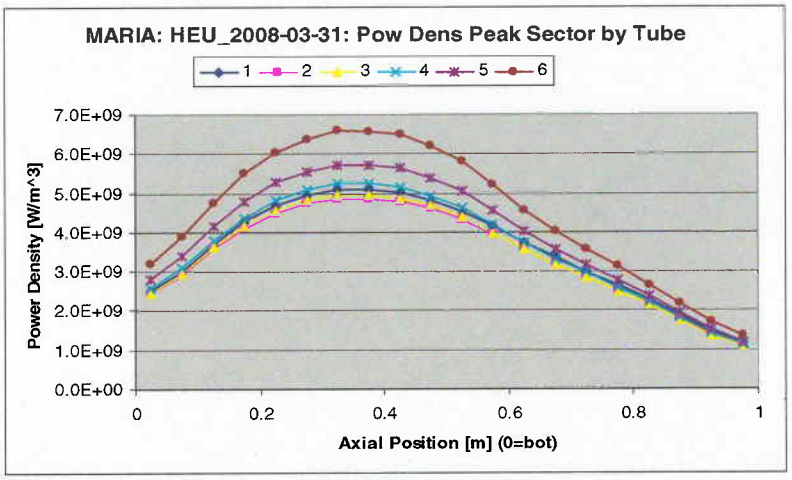

Figure 3.1.2 Power Density in Peak Sector of HEU FA in HEU Core

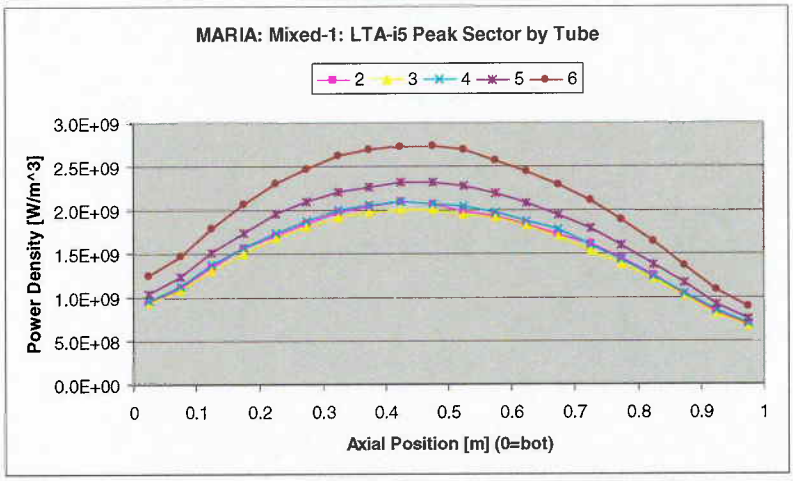

Figure 3.1.3 Power Density in Peak Sector of LTA-1 in HEU+LTA-i5 Core

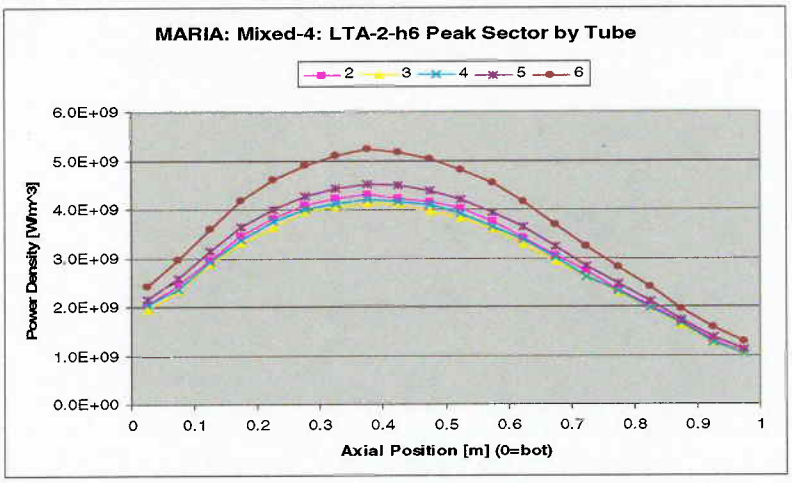

Figure 3.1.4 Power Density in Peak Sector of LTA-2 in HEU+LTA-h6-h7 Core

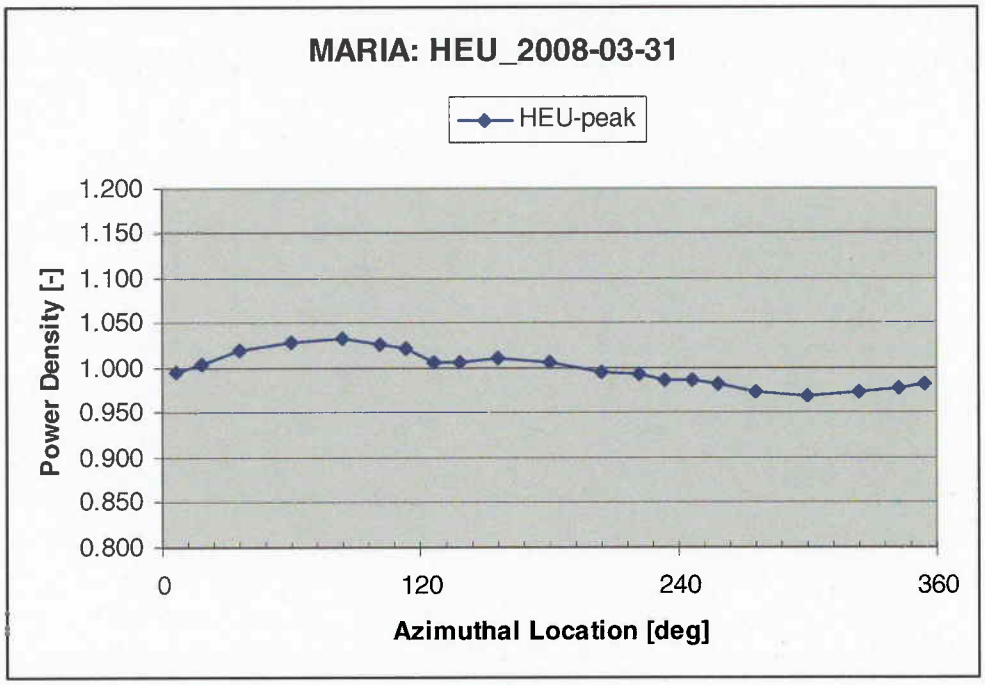

Figure 3.1.5 Relative Power Density vs. Azimuthal Position in one FA at 0.325 m Above Bottom in HEU Core

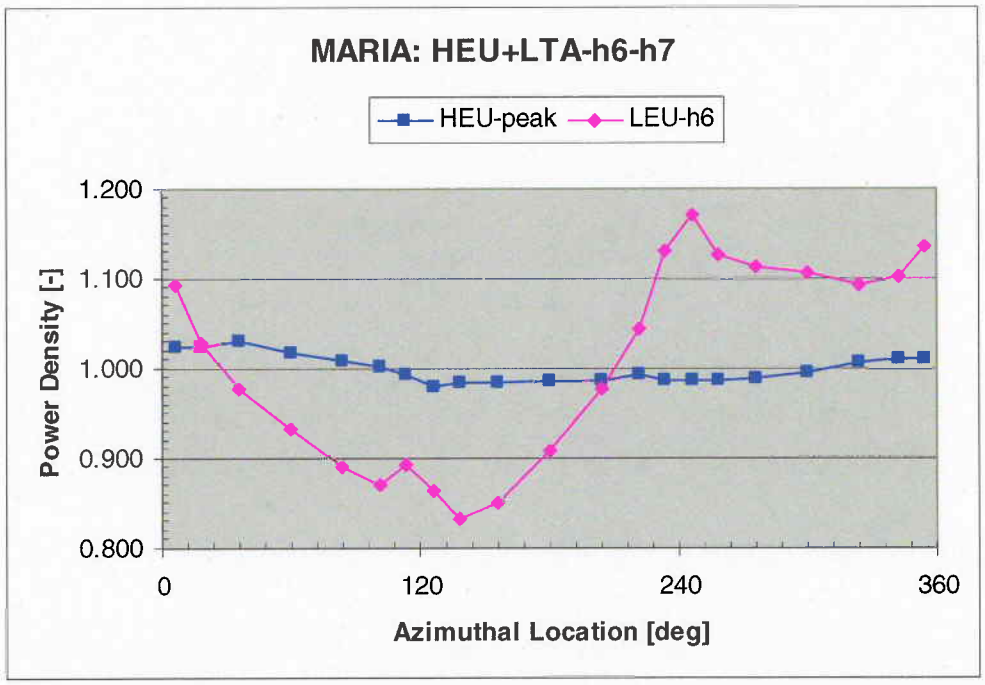

Figure 3.1.6 Relative Power Density vs. Azimuthal Position in two FA at 0.375 m Above Bottom in HEU+LTA-h6-h7 Core

3.2. Assessment of Model

Thermal-hydraulic modeling of research reactor core conversions requires making approximations. A typical approach is to divide the core into a hot channel and an average channel, where a "channel" may be anything from a fraction of a fuel assembly up to multiple fuel assemblies. The hot channel is typically a portion of the fuel having the peak power density and is used to assess maximum temperatures, at steady state and during transients. The average channel represents the rest of the core and is the basis for temperature-based feedbacks in the reactor kinetics calculations. Reference 7 demonstrated the success of this technique as applied to IRT-3M and IRT-4M fuel assemblies, which are composed of concentric square fuel tubes.

A similar assessment has been performed for the MARIA reactor fuel. The process was to compare a two-dimensional RELAP-5 model with a three-dimensional model in STAR-CD [Ref. 8]. The specific power, temperature, and flow rate values used in this section are different from those used in the LTA calculations shown in other sections of this report because this assessment was performed for the HEU FA and LEU LTA in different core configurations.

Comparison between the RELAP5 and STAR-CD model assumptions is provided here. Each fuel tube in the RELAP5 model is a "heat structure" and allows heat transfer in one-dimension, which is radial, to the coolant on both sides. The coolant flow in RELAP5 is one-dimensional, which is axial in the gap between adjacent fuel tubes. A mixture of zero- and one-dimensional plena at the top and bottom of the fuel tubes in RELAP5 disperse and collect flow between the tube gaps. The model in STAR-CD is fully three dimensional, which adds details such as axial and azimuthal conduction within fuel tubes, radial and azimuthal distribution of velocity and temperature in the coolant, and spatial details of coolant mixing in the plena. The RELAP5 calculations were done using two different sold-fluid heat transfer correlations: Dittus-Boelter (denoted "D-B" in figures), which is the default, and Petukov (denoted "Pet" in the figures), which has been suggested as applicable for parallel plate geometry. No such choice is needed in STAR-CD, which computes the heat transfer on a somewhat "first-principles" basis.

A 60-degree sector of the MARIA FA was felt to be sufficient for the model within STAR-CD. Figure 3.2.1 shows an overall view of the STAR-CD model; the upper part of the FA is on the left side of the figure, showing the extension above tube 4 being used to divide downward flow on the outside from upward flow on the inside; the lower part of the FA is on the right side of the figure, showing that the bottom of tube 4 is lower than the other tubes, which forces the coolant flow to continue downward an additional distance (which promotes mixing) before turning to flow upward.

A cross section through the STAR-CD model of the HEU FA is shown on the left side of Figure 3.2.2 and for the LEU FA on the right side. Notable differences between the two FA are fuel meat is thicker in the LEU, clad is thinner in the LEU, 1 less fuel tube in the LEU, fuel meat is not azimuthally continuous in the LEU, and the tube stiffener in the LEU is larger than the rib on the tubes in the HEU.

The HEU FA was analyzed for a fresh FA in position h-7 of the May 16, 2006 core. The 24-degree sector having the peak power density (6094 MW/m^3) in MCNP was used to prepare power data for the RELAP5 model; this resulted in a FA power of 1.42 MW. The 60-degree sector containing the 24-degree peak power density node was used in the STAR-CD model; the azimuthal power variation in this 60-degree sector was ±1%. For both codes the inlet temperature was 60°C (333 K) and the coolant flow rate was 25 m^3/h per FA. Figure 3.2.3 shows the temperatures calculated using both codes at the axial location of peak power density. The horizontal axis scale of 1 to 25 is as follows: 1 is the coolant interior to tube 1; 2, 3, 4, and 5 are the inner clad surface, fuel maximum, outer clad surface, and coolant outside for tube 1; 6 through 9 repeat these for fuel tube 2; 10 through 13 repeat these for tube 3, 14 through 17 repeat these for tube 4, 18 through 21 repeat these for tube 5, and 22 through 25 repeat these for tube 6. Fuel tube temperatures computed using Dittus-Boelter heat transfer correlation are always higher than the temperatures calculated using the Petukov correlation, although the spread is less than 5°C for this case. The two RELAP5 calculations with different heat transfer correlations essentially bracket the STAR-CD results.

The LEU FA was analyzed for a power distribution provided to the fuel designer by IAE [Ref. 9] in which each 120-degree sector was divided into 3 40-degree nodes. The 40-degree node having the peak power density (6046 MW/m^3) was used to prepare power data for the RELAP5 model; this resulted in a FA power of 2.0 MW. The 60-degree sector containing the peak power density node was used in the STAR-CD model; the azimuthal power variation in this 60-degree sector was ±1.4%. For both codes the inlet temperature was 50°C (323 K) and the coolant flow rate was 25 m^3/h per FA. Figure 3.2.4 shows the temperatures calculated using both codes at the axial location of peak power density. The horizontal axis scale of 1 to 21 is as follows: 1 is the coolant interior to tube 2; 2, 3, 4, and 5 are the inner clad surface, fuel maximum, outer clad surface, and coolant outside for tube 2; 6 through 9 repeat these for fuel tube 3; 10 through 13 repeat these for tube 4, 14 through 17 repeat these for tube 5, and 18 through 21 repeat these for tube 6. Fuel tube temperatures computed using Dittus-Boelter heat transfer correlation are always higher than the temperatures calculated using the Petukov correlation, although the spread is less than 10°C for this case. The two RELAP5 calculations with different heat transfer correlations bracket the STAR-CD results for tubes 4-6 and are close for the tubes 2-3.

There are additional results shown for the LEU case. Figure 3.2.5 shows coolant temperature at the "tube exit", which is at the top of the tubes for coolant interior to tube 4 and at the bottom of the tubes for coolant outside of tube 4; there is excellent agreement (i.e., within 1 to 2°C) among the 2 RELAP5 cases and STAR-CD (i.e., comparing the solid and dashed lines); STAR-CD shows within-channel variation of 12 to 27°C (i.e., using the chain-dash lines). Figure 3.2.6 shows that there is azimuthal variation within fuel, clad, and coolant in this case even though the azimuthal power distribution is quite uniform; this is caused by the azimuthal discontinuity of the fuel meat combined with the stiffener, which acts as a fin for heat transfer purposes; azimuthally, the power density peaks near the stiffener but the temperature peaks away from the stiffener.

There is no experiment data for these FA upon which to base a decision about which heat transfer correlation to use in RELAP5. Since Dittus-Boelter give higher clad temperatures than Petukov, the rest of the analysis has been performed using the Dittus-Boelter heat transfer correlation; that choice is conservative for safety analysis purposes.

These calculations comparing RELAP5 with STAR-CD provide a high confidence that modeling the peak power sector using RELAP5 with the Dittus-Boelter heat transfer correlation will provide an adequate approximation for peak clad temperature in the HEU and LEU FA for MARIA.

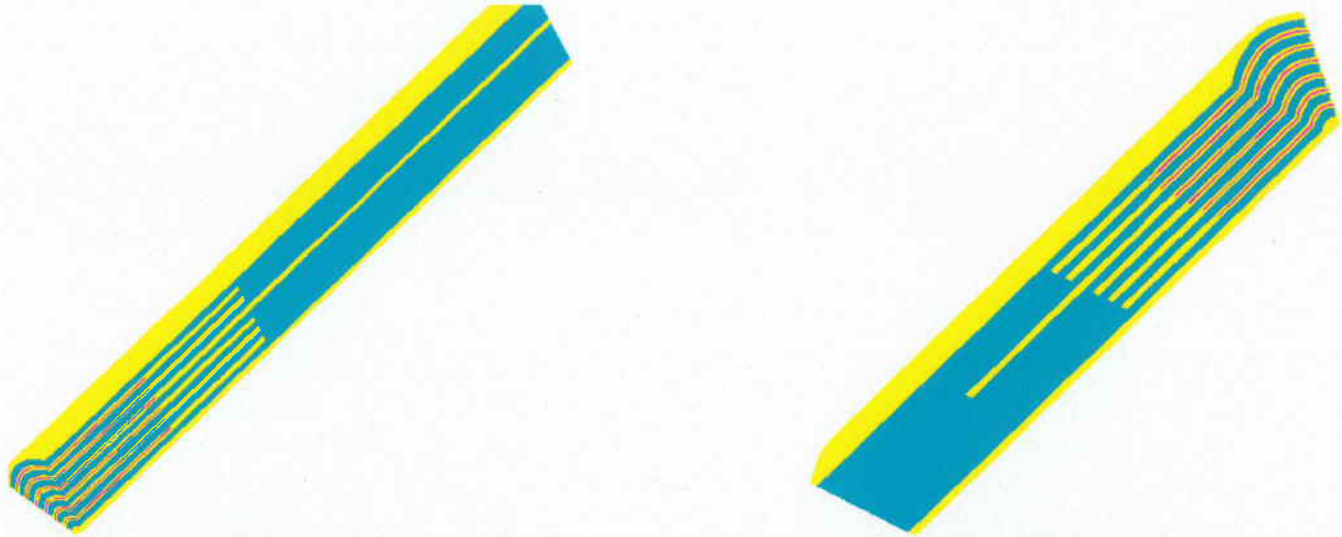

Figure 3.2.1 Overall STAR-CD Model of HEU FA (top portion of FA is on left, bottom of FA is on right) Colors used hei and Figure 3.2.2 are blue for coolant, yellow for clad and structure, orange for non-clad structure, and red for fuel meat.

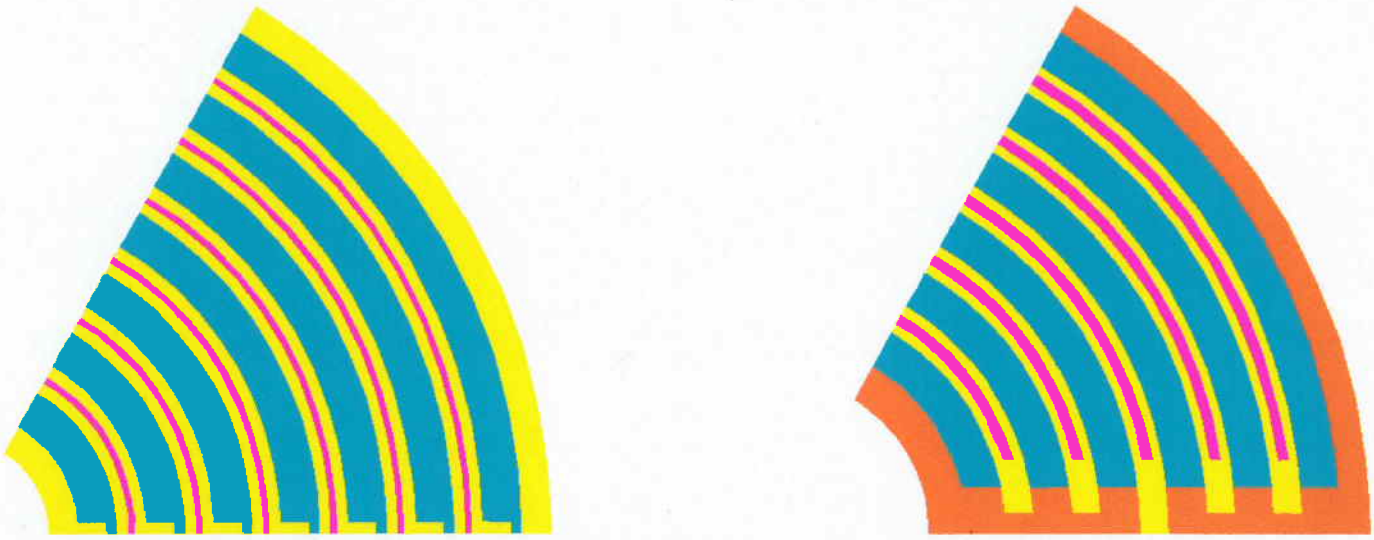

Figure 3.2.2 Radial-Azimuthal STAR-CD Model of HEU (left) and LEU (right) FA

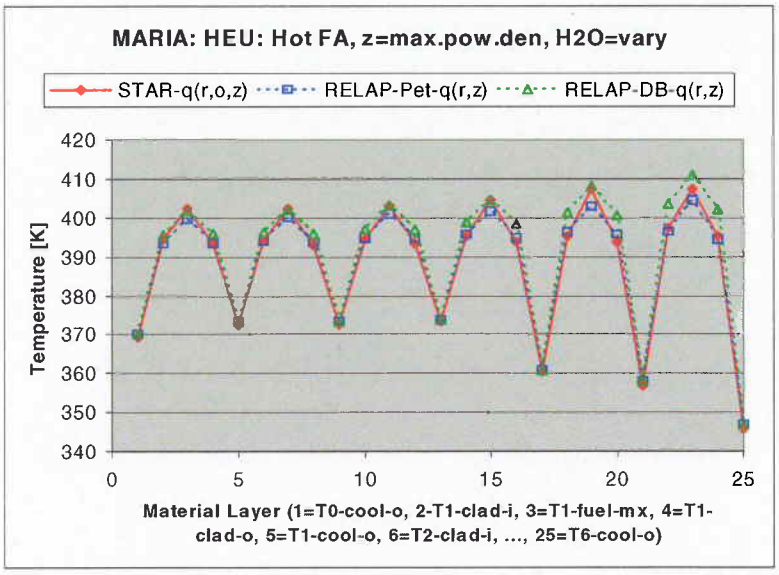

Figure 3.2.3 Temperature at Height of Peak Power Density in HEU FA

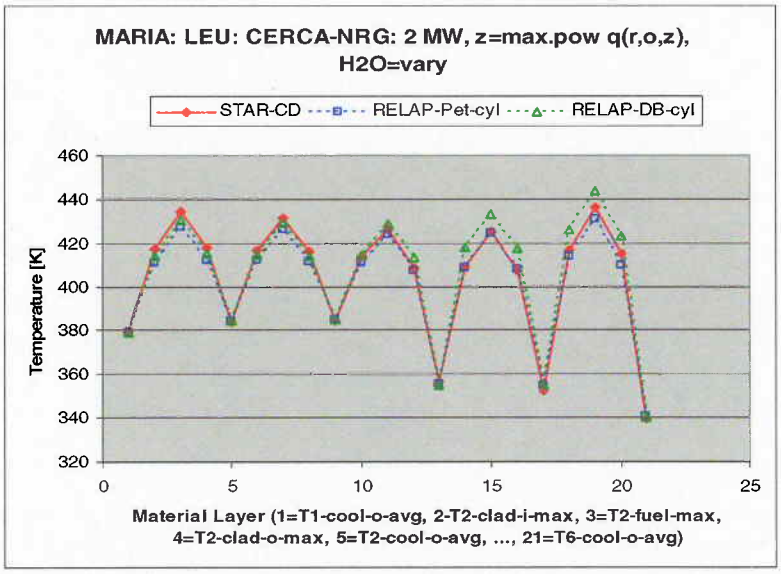

Figure 3.2.4 Temperature at Height of Peak Power Density in LEU FA

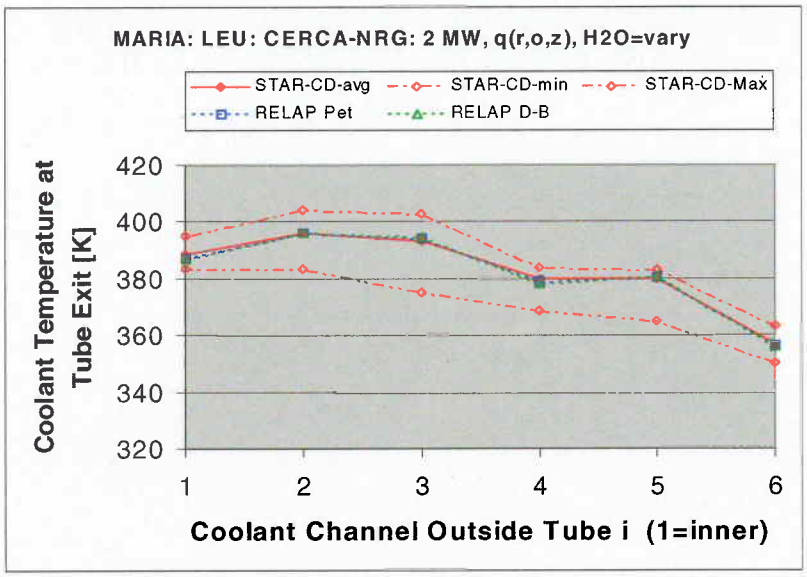

Figure 3.2.5 Temperature of "Exit" Coolant in LEU FA

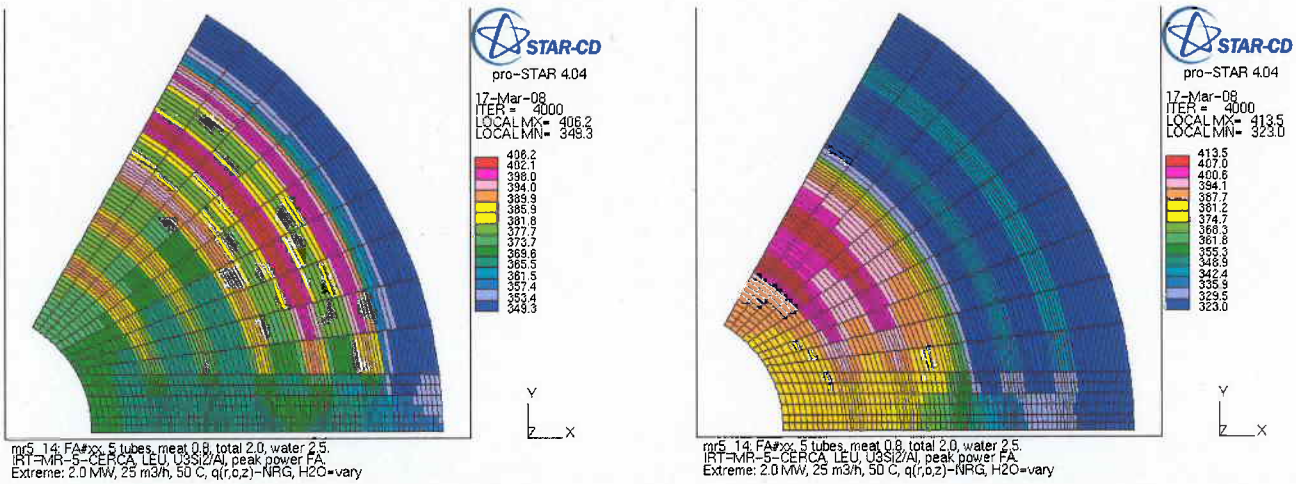

Figure 3.2.6 Temperature Distribution in LEU FA at Bottom (left) and Top (right) of Fuel Meat

3.3. Evaluation Basis and Hot Channel Factors

IAE has specified two criteria against which steady-state results with the hot channel factors combined statistically are to be checked for the maximum power allowed for a specific flow rate: (1) The peak clad surface temperature must be less than the local coolant saturation temperature; and (2) the onset of nucleate boiling ratio (ONBR) must be greater than 1.2, where

$$ONBR = (T_{ONB} - T_{in}) / (T_{wall} - T_{in}) \quad (3.3.1)$$

and the temperature for the onset of nucleate boiling is computed from a correlation attributed to Forster-Greif [Ref. 10]

$$T_{ONB} = T_{sat} + 0.182 * q^{0.35} / P^{0.23} \quad (3.3.2)$$

where T_{in} is inlet coolant temperature, T_{wall} is the wall surface temperature, T_{sat} is saturation coolant temperature, q is heat flux [W/m^2], and P is pressure [bar]. (Temperatures must all be in the same units, either [K] or [°C].) These two criteria will allow IAE to define different operating conditions. By way of comparison, in the 1999 SAR for the MARIA reactor the criterion used is maximum clad temperature less than 180°C with hot channel factors combined statistically and multiplicatively.

Steady-state reactor calculations are typically done for nominal conditions and for a second set of conditions which include uncertainty or "hot channel" factors. Examples of uncertainties are manufacturing tolerances (e.g., fuel meat thickness, coolant gap thickness) and measurement errors during operation. The intent is to systematically allow for combinations of these uncertainties in establishing the operating envelope for the FA. The base data for the hot channel factors for the HEU FA was taken from Section 5.4 the SAR and are shown in Table 3.3.1. The only known change to these values for the LEU FA is the increase in the fuel distribution nonuniformity (i.e., "A" in Table 3.3.1) to 1.20 (from 1.15) representing the allowed manufacturing tolerance in the fuel design agreed between IAE and CERCA.

The resulting hot channel factors are shown in Table 3.3.2 for the HEU FA and in Table 3.3.3 for the LEU FA. The methodology for the use of the hot channel factors is described in [Ref. 11]. For the steady-state evaluation, coolant flow rate is defined to be 90% of the nominal value (i.e., 22.5 m^3/h for HEU FA and 23.4 m^3/h for LEU FA), since the flow can decrease to this point without any alarm being generated.

Table 3.3.1 Components of HEU Hot Channel Factors

Description	Value
Non-uniformity of the fuel distribution along the fuel element	A = 1.15
Inaccuracy of the formula for the heat transfer coefficient	B = 0.90
Diminishing of the fuel transfer surface due to decrease of the fuel layer thickness under the rib; this coefficient always exists and it should be treated rather as a correction factor which is not resulted from the non-uniformity	C = 0.95
Deviations of the fuel tube diameters equating 0.3%	neglect
Inaccuracy of determining the fuel layer length in fuel element for the minimum length of 95 cm (only the measurement accuracy should be taken into account); the error doesn't exceed 1%, hence:	D = 0.99
Decrease of the hydraulic diameter of the water channel between neighbouring fuel tubes, to be determined by a possible deviation of all tubes in one side to the ultimate position due to the rib location	E = 0.8
Channel power to be determined based on flow rate measurement and water heating up	F = 1.02
Measurement errors don't exceed 2%	G = 1.02
Fuel contents in the separate tubes may differ within the bounds of 2% from the nominal value	H = 1.02
Axial non-uniformity coefficient of fuel distribution doesn't exceed 3%	I = 1.03

Table 3.3.2 Hot Channel Factors for HEU FA

uncertainty	effect on bulk ΔT, fraction	toler-ance, fraction	heat flux, F_q	channel temper-ature rise, F_{bulk}	film temper-ature rise, F_{film}
random errors					
fuel meat thickness (local)		0.15	1.15		1.15
U235 homogeneity (local)		0.03	1.03		1.03
U235 loading per plate	0.50	0.06	1.06	1.030	1.06
power density	0.50	0.00	1.00	1.000	1.00
channel spacing	1.00	1.20		1.37	1.07
flow distribution	1.00	0.00		1.00	1.00
random errors combined			**1.16**	**1.37**	**1.18**
systematic errors					
power measurement	1.00	**0.07**			
flow measurement	1.00	**0.02**			
heat transfer coefficient		**0.10**			

Table 3.3.3 Hot Channel Factors for LEU FA

uncertainty	effect on bulk ΔT, fraction	toler-ance, fraction	heat flux, F_q	channel temper-ature rise, F_{bulk}	film temper-ature rise, F_{film}
random errors					
fuel meat thickness (local)		0.20	1.20		1.20
U235 homogeneity (local)		0.03	1.03		1.03
U235 loading per plate	0.50	0.06	1.06	1.030	1.06
power density	0.50	0.00	1.00	1.000	1.00
channel spacing	1.00	1.20		1.37	1.07
flow distribution	1.00	0.00		1.00	1.00
random errors combined			**1.21**	**1.37**	**1.22**
systematic errors					
power measurement	1.00	**0.07**			
flow measurement	1.00	**0.02**			
heat transfer coefficient		**0.10**			

3.4. Results

A summary of the steady-state results is presented in Table 3.4.1. The peak clad temperature usually occurs near the location of peak power density. For these FA the peak clad temperature occurs on the interior of tube 6 (which is in the downflow coolant section). For the HEU core the nominal peak value is 136.3°C. The peak clad temperature decreases (by up to 6°C) in the HEU part of the other 4 cores due to there being a lower power in the peak HEU FA in these cores. The nominal peak clad temperature in the LEU LTAs is 144.7°C (or about 8°C higher than the highest nominal HEU value) in the core with both LTAs in high power positions.

As shown in Table 3.4.1 the use of the hot channel factors (combined statistically) increases the peak clad temperature. In this case the peak clad temperature is equal to 170.3°C for the HEU FA and equal to 186.7°C for the peak LEU LTA.

To put these clad temperatures in perspective it is noted that they are less than the saturation temperature of about 202°C.

The ONBR was computed only with hot channel factors included. The minimum value of ONBR is 1.36 for the HEU core. The minimum ONBR increases to 1.45 in the HEU portion of the other 4 cores. The minimum value of ONBR is 1.24 in the LEU LTA portion of the core with both LTAs in high power positions. All of these values are acceptable relative to the minimum acceptable value of 1.2 (which in principle is the criterion to be used by IAE).

The following observation on Table 3.4.1 is important because it shows the importance of the azimuthal power density distribution. The bottom 2 rows of Table 3.4.1 provide some indication of the azimuthal power density distribution with a FA. The value before the "/" is the power generated in the FA as calculated using MCNP (i.e., using the actual azimuthal distribution). The value after the "/" is the power generated in the FA when power densities in the peak sector (either 12 or 24 degrees azimuthally) are used in the full FA circumference. There is essentially no difference between these two powers for the peak HEU FA, indicating that there is very little azimuthal power variation. The two powers differ by 15 to 19% for the LEU LTA, indicating a rather prominent azimuthal power variation. A portion of the variation is due to the fuel not being continuous azimuthally in the LEU LTA.

Examples of the hot surface clad temperature variation axially are provided in Figures 3.4.1 and 3.4.2.

The next two figures are the result of using the acceptance criteria (described above) to establish an operating envelope. Each line was obtained by adjusting the FA power in order to match either the T_{sat} limit (for one curve in a pair) or ONBR limit (for the other curve in a pair). Figure 3.4.3 shows results with no hot channel factors. For the HEU FA with nominal flow rate of 25 m^3/h, the T_{sat} limit is satisfied if the power is less than 3.1 MW per FA and the ONBR limit is satisfied if the power is than 2.8 MW per FA. For the LEU LTA with nominal flow rate of 26 m^3/h, the T_{sat} limit is satisfied if the power is less than 2.5 MW per FA and the ONBR limit is satisfied if the power is than 2.3 MW per FA. If the flow rate is lower (or higher) then the

allowed power is lower (or higher). Anywhere below each line will result in operation within the allowed criteria. The ONBR limit is seen to be more restrictive than the T_{sat} limit. The LEU LTA must operate at a lower power than the HEU FA to satisfy these limits.

Inclusion of hot channel factors imposes an operating restriction, as shown in Figure 3.4.4. The HEU FA at nominal flow rate is limited to 2.1 MW using the T_{sat} criterion and to 1.9 MW using the ONBR criterion; both of these are substantial reductions below the 3.1 and 2.8 MW values without hot channel factors but are not overly restrictive since nominal FA power is less than 2 MW. The lower 2 lines in Figure 3.4.4 are for the LEU LTA; for a nominal coolant flow rate of 26 m^3/h, the power must be less than 1.6 MW per FA to satisfy the T_{sat} limit and less than 1.5 MW per FA to satisfy the ONBR limit. The fact that the LEU LTA operating power per FA is substantially less than that allowed for the HEU FA may restrict the operating capability of the reactor.

Table 3.4.1 Summary of Steady-State Results

	Core Configuration				
	HEU Core	LTA in i-5	LTA in h-7	LTA in i-5 & h-7	LTA in h-6 & h-7
Peak HEU FA Clad Temperature [°C]:					
Nominal	136.3	131.4	130.8	130.2	129.8
With Hot Channel Factors (statistically combined)	170.8	164.7	164.5	164.0	163.2
ONBR (with Hot Channel Factors)	1.36	1.43	1.44	1.44	1.45
Peak LTA Clad Temperature [°C]:					
Nominal		104.0	139.1	138.4	144.7
With Hot Channel Factors (statistically combined)	N/A	128.3	178.6	177.5	186.5
ONBR (with Hot Channel Factors)		2.11	1.31	1.32	1.24
Power Generated in Peak FA [MW]:					
HEU (MCNP/Using Peak Segment)	1.64/1.65	1.60/1.60	1.59/1.59	1.56/1.56	1.56/1.56
LTA (MCNP/Using Peak Segment)	N/A	0.75/0.89	1.31/1.52	1.28/1.47	1.44/1.66

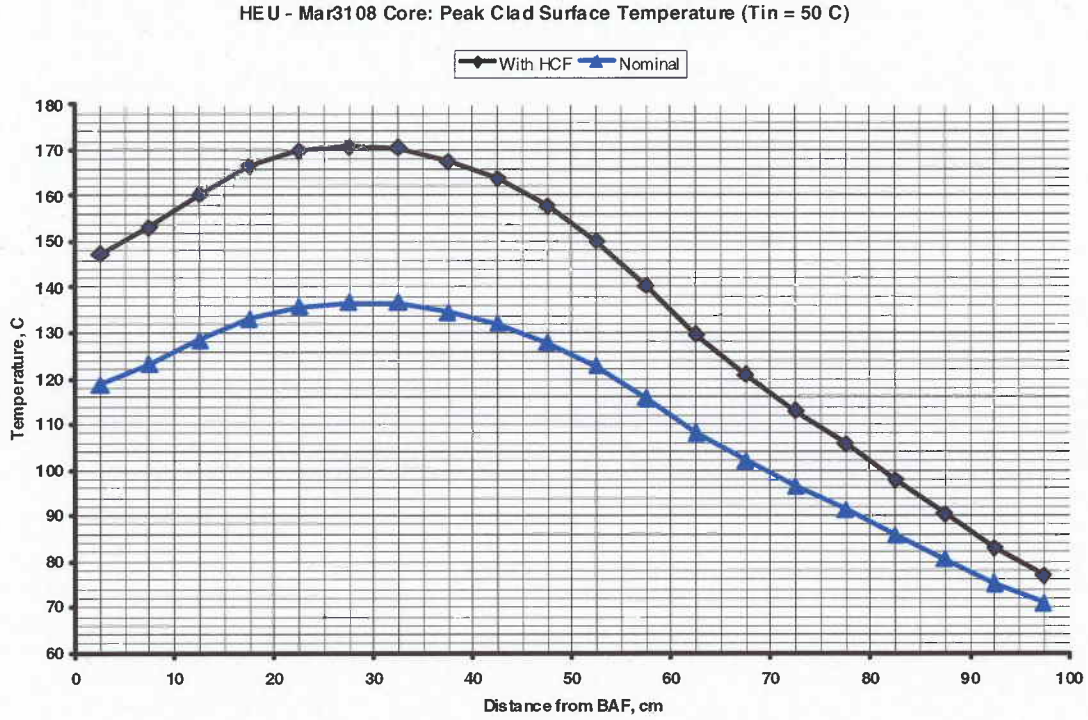

Figure 3.4.1 Peak Clad Surface Temperature for HEU Core

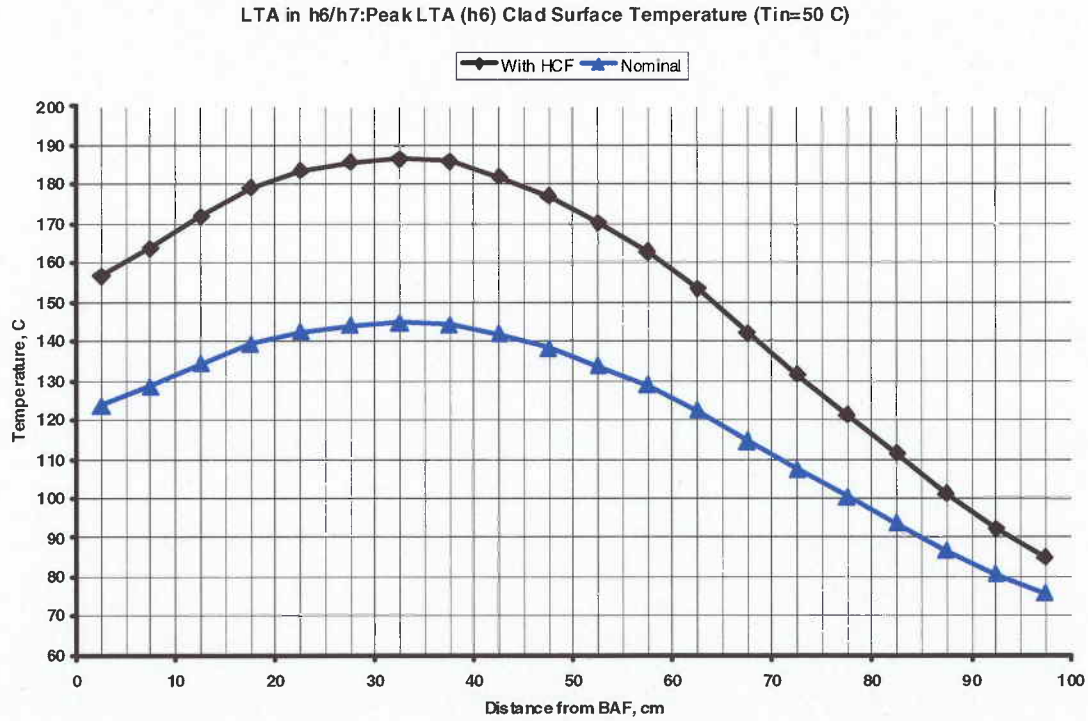

Figure 3.4.2 Peak Clad Surface Temperature in LTA

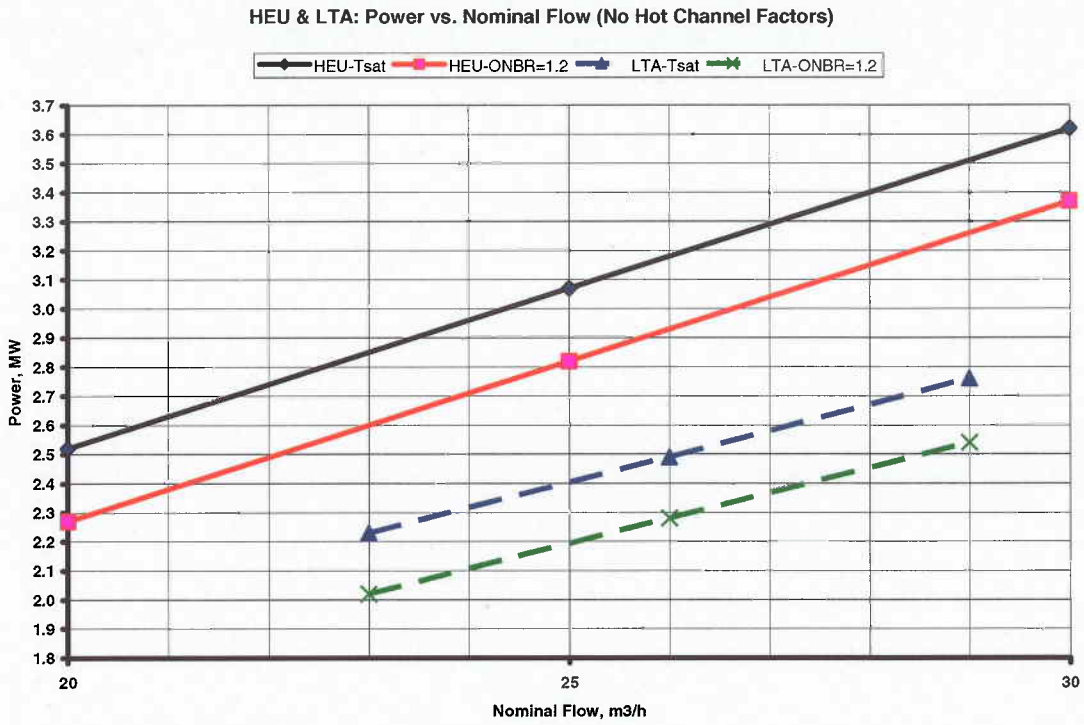

Figure 3.4.3 Allowed Power vs. Flow Rate without Hot Channel Factors

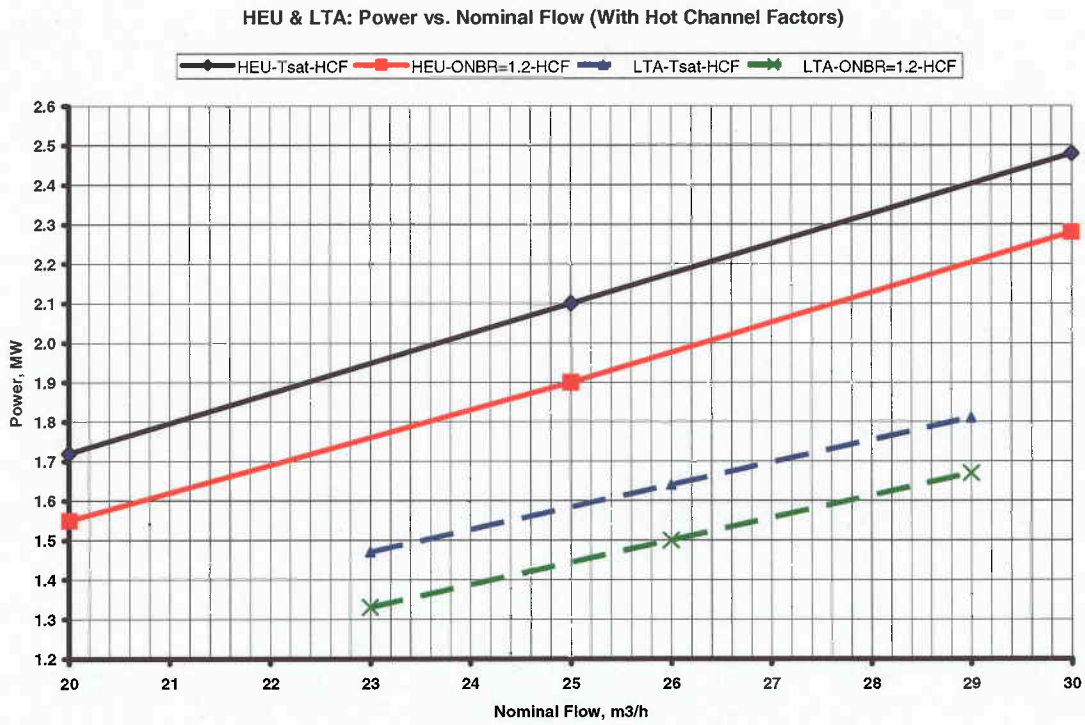

Figure 3.4.4 Allowed Power vs. Flow Rate with Hot Channel Factors

4. Transient Analysis

In addition to satisfying steady state criteria, the behavior of the LTAs must be examined for various transients. Three reactivity-initiated events are considered: cold water injection (cf. Sec. 4.2), fast reactivity insertion (cf. Sec. 4.3), and slow reactivity insertion (Sec. 4.4). The transients are considered for all 5 core configurations and presented in the following order: all HEU, LTA in i5, LTA in h7, LTA in i5 and h7, and LTA in h6 and h7 . The transients are discussed in the indicated sections after the conditions common to all cases are presented in Section 4.1.

4.1. Common Conditions

All transients start from steady state. Only the core is required to be modeled for these transients due to their short time span. All 5 core configurations were considered. Coolant flow rate is nominal and the inlet temperature is 323 K (50°C). Each transient is started from two different powers: (1) low power of 10 kW (i.e., at just critical) and (2) nominal operating power of 16 MW.

The reactivity transients are all terminated by scram on high power. The main high power trip is on 120% of 16 MW or 19.2 MW. Operationally, the power scale maximum is reset at 80% of maximum scale to 25% during power ascension phase; the scram is at 120% of maximum scale; therefore, it is also necessary to allow in calculations starting from low power for scram to occur at (120/25)*10 kW or 48 kW. There are other possible scrams (e.g., low period, low flow, high temperature) in MARIA; all of these are ignored in the present analysis.

After a scram setpoint has been crossed, there is a 0.2 s delay after which the control rods begin to fall by gravity into the reactor core in order to stop the nuclear fission chain reaction. The scram process inserts approximately 15 $ of negative reactivity in 0.64 s; the actual reactivity insertion versus time is computed by combining total worth less one stuck rod in the bottom row of Table 2.4.4 with the control rod worth versus position in Figures 2.4.3-2.4.5 and the rod position versus time in Figure 2.4.6. The primary pumps continue to run after scram.

4.2. Cold Water Injection

4.2.1. Boundary Conditions

This transient represents a sudden decrease in inlet temperature. A mechanistic basis that would cause this to happen is not specified. A decrease in inlet temperature leads to a positive reactivity insertion since the reactivity feedback coefficients for temperature are negative in the fuel channel cooling loop. Although inlet temperature can be a function of time in the RELAP5 model, the inlet temperature decrease was modeled as being equivalent to a 0.8 $ reactivity insertion with inlet temperature held constant; with a coolant temperature reactivity feedback coefficient of 0.023-0.024 $/°C and a void reactivity coefficient of 0.063-0.081 $/% of void, the 0.8 $ reactivity is equivalent to a temperature decrease of about 30°C. The insertion was assumed to be in a single step (actually over 0.05 s in the calculation).

4.2.2. Results

The results computed using RELAP5 for this transient starting from low power in the HEU core are shown in Figure 4.2.2.1. The step reactivity addition causes the power to rise, crossing the 48 kW scram setting at about 0.25 s. The control rods start moving into the core 0.2 s later, at which time the power peaks at about 64 kW. By 0.6 s the power is less than the initial value and continues decreasing. The peak cladding temperature is 50.3°C at peak power and has decreased to less than the initial value after 0.8 s; no clad damage would be expected based on these temperature changes. Figure 4.2.2.1.c shows the reactivity addition over 0.05 s and essentially no reactivity feedbacks until scram, which is -15 $ in 0.64 s. With the reactor subcritical and temperatures decreasing there is no need to consider a longer time span than that shown here for this case.

The results computed for this transient starting from high power in the HEU core are shown in Figure 4.2.2.2. The step reactivity addition causes the power to rise, crossing the 19.2 MW scram setting in about 0.02 s. The control rods start moving into the core 0.2 s later, at which time the power had already peaked at 52 MW. By 0.3 s the power is less than the initial value and continues decreasing. The peak cladding temperature is 226°C at its peak and has decreased to less than the initial value after 0.45 s; no clad damage would be expected based on these temperature changes. Figure 4.2.2.2.c shows the reactivity addition over 0.05 s, a small decrease in reactivity as temperature rises, and insertion of the scram reactivity, which is -15 $ in 0.64 s. With the reactor subcritical and temperatures decreasing there is no need to consider a longer time span than that shown here for this case.

The results are shown in Figures 4.2.2.3 and 4.2.2.4 for the core with LTA in i-5, in Figures 4.2.2.5 and 4.2.2.6 for the core with LTA in h-7, in Figures 4.2.2.7 and 4.2.2.8 for the core with LTA in i-5 and h-7, and in Figures 4.2.2.9 and 4.2.2.10 for the core with LTA in h-6 and h-7. The following discussion will only highlight differences among these cores.

For the cases starting at low power there is essentially no difference in peak power or its timing except for the core with LTA in h-6 and h-7, where the peak power is 60 kW instead of 64-

65 kW at 0.6 s instead of 0.45 s. The peak clad temperature is less that 50.4°C for all cores; the peak clad temperature is slightly higher or lower reflecting the differences in the peak power density at steady state.

For the cases starting at high power, the peak power varies from 50 to 55 MW at about 0.2 s. The peak clad temperature in the HEU FA having the peak power density ranges from 215-226°C. The peak clad temperature in the LEU LTA ranges from 172-237°C which reflects the differences in steady-state temperatures which are due to the differences in peak power density. For the core with LTA in h-6 and h-7, the peak clad temperatures in the LTAs are higher than the peak in the HEU FA. The maximum clad temperatures during this transient are very far from the clad damage temperature.

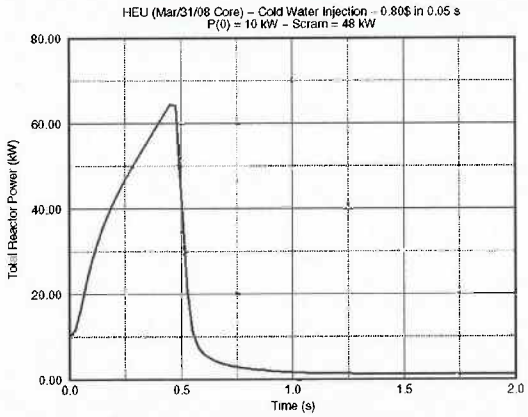

Figure 4.2.2.1.a Power vs. Time for Cold Water Injection (0.8 $ Step) at 10 kW in HEU Core

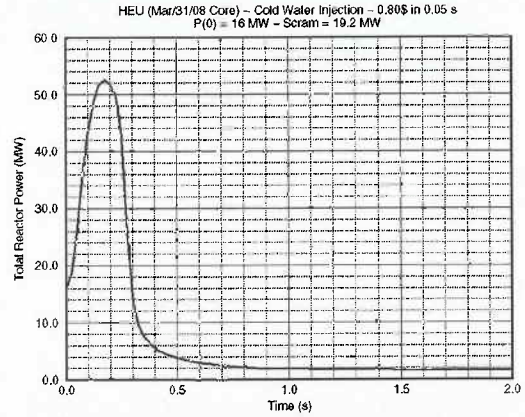

Figure 4.2.2.2.a Power vs. Time for Cold Water Injection (0.8 $ Step) at 16 MW in HEU Core

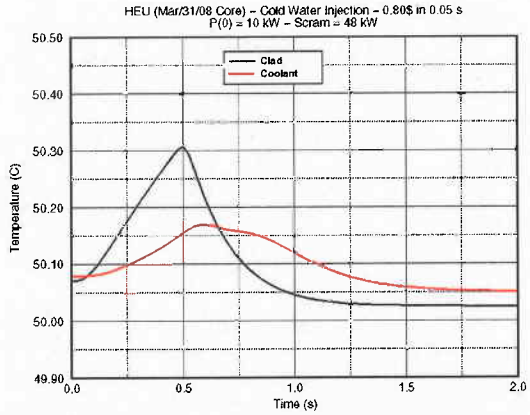

Figure 4.2.2.1.b Temperature vs. Time for Cold Water Injection (0.8 $ Step) at 10 kW in HEU Core

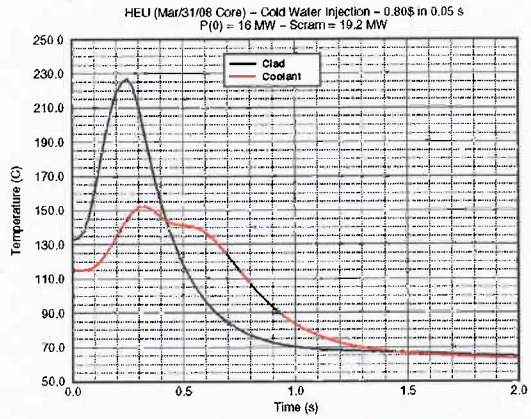

Figure 4.2.2.2.b Temperature vs. Time for Cold Water Injection (0.8 $ Step) at 16 MW in HEU Core

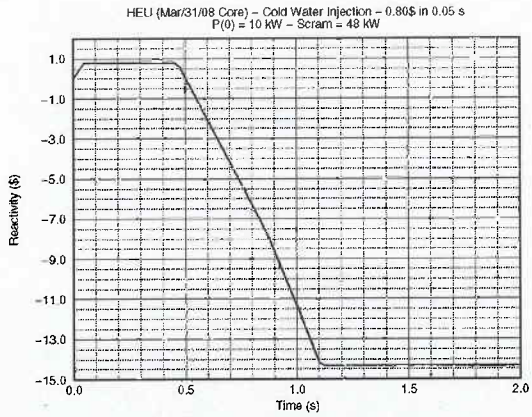

Figure 4.2.2.1.c Net Reactivity vs. Time for Cold Water Injection (0.8 $ Step) at 10 kW in HEU Core

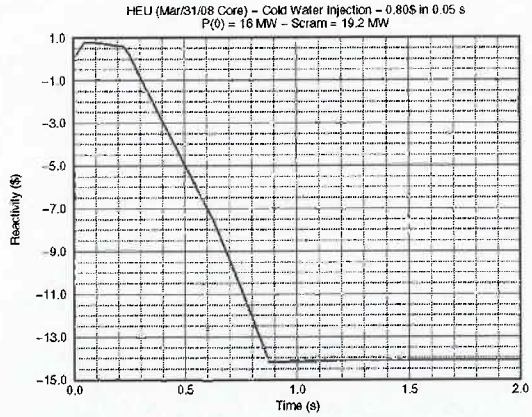

Figure 4.2.2.2.c Net Reactivity vs. Time for Cold Water Injection (0.8 $ Step) at 16 MW in HEU Core

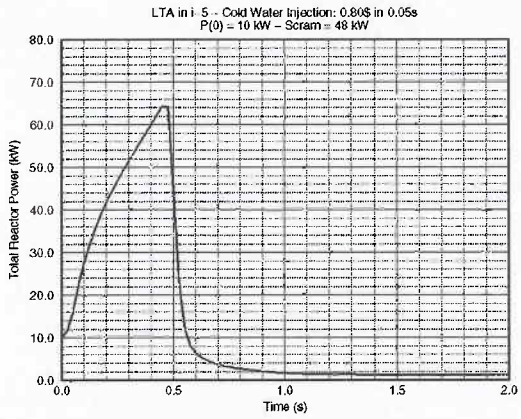

Figure 4.2.2.3.a Power vs. Time for Cold Water Injection (0.8 $ Step) at 10 kW in HEU+LTA-i5 Core

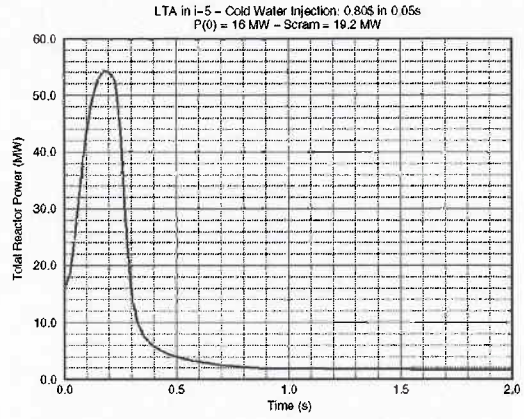

Figure 4.2.2.4.a Power vs. Time for Cold Water Injection (0.8 $ Step) at 16 MW in HEU+LTA-i5 Core

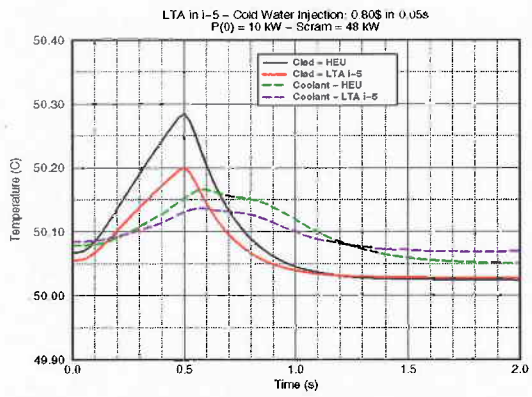

Figure 4.2.2.3.b Temperature vs. Time for Cold Water Injection (0.8 $ Step) at 10 kW in HEU+LTA-i5 Core

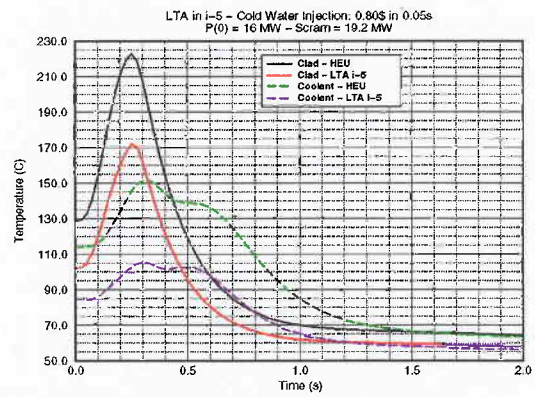

Figure 4.2.2.4.b Temperature vs. Time for Cold Water Injection (0.8 $ Step) at 16 MW in HEU+LTA-i5 Core

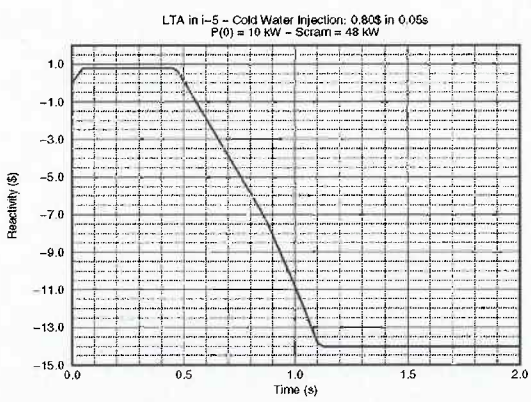

Figure 4.2.2.3.c Net Reactivity vs. Time for Cold Water Injection (0.8 $ Step) at 10 kW in HEU+LTA-i5 Core

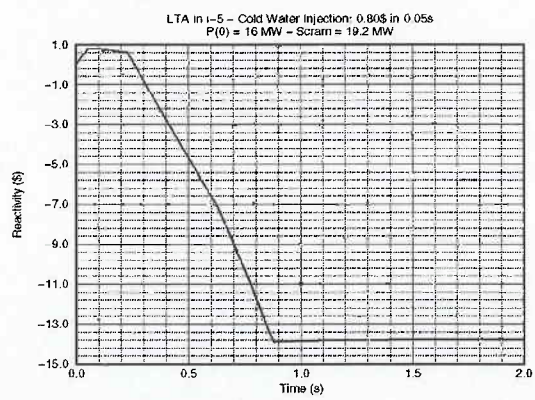

Figure 4.2.2.4.c Net Reactivity vs. Time for Cold Water Injection (0.8 $ Step) at 16 MW in HEU+LTA-i5 Core

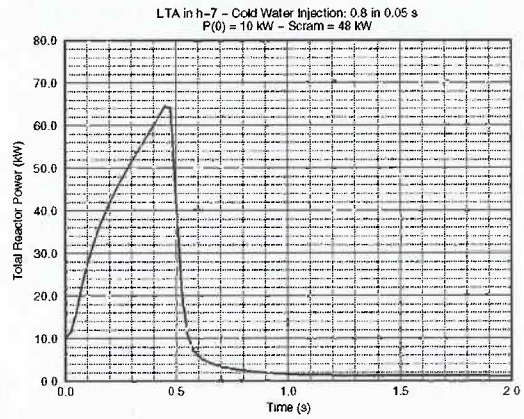

Figure 4.2.2.5.a Power vs. Time for Cold Water Injection (0.8 $ Step) at 10 kW in HEU+LTA-h7 Core

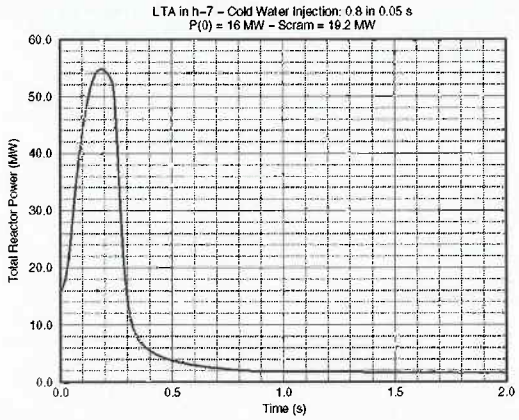

Figure 4.2.2.6.a Power vs. Time for Cold Water Injection (0.8 $ Step) at 16 MW in HEU+LTA-h7 Core

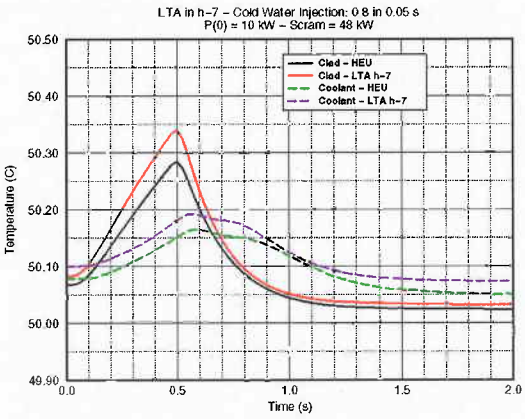

Figure 4.2.2.5.b Temperature vs. Time for Cold Water Injection (0.8 $ Step) at 10 kW in HEU+LTA-h7 Core

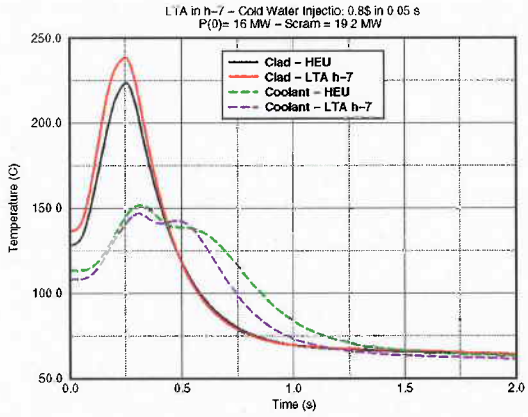

Figure 4.2.2.6.b Temperature vs. Time for Cold Water Injection (0.8 $ Step) at 16 MW in HEU+LTA-h7 Core

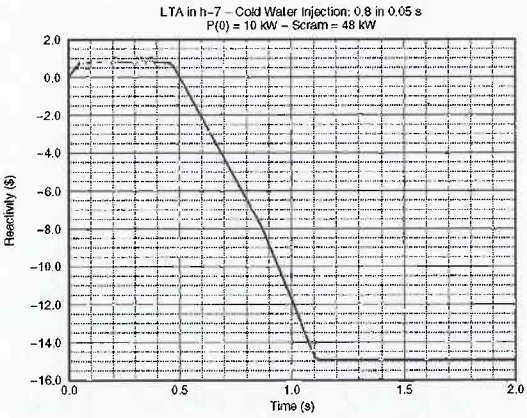

Figure 4.2.2.5.c Net Reactivity vs. Time for Cold Water Injection (0.8 $ Step) at 10 kW in HEU+LTA-h7 Core

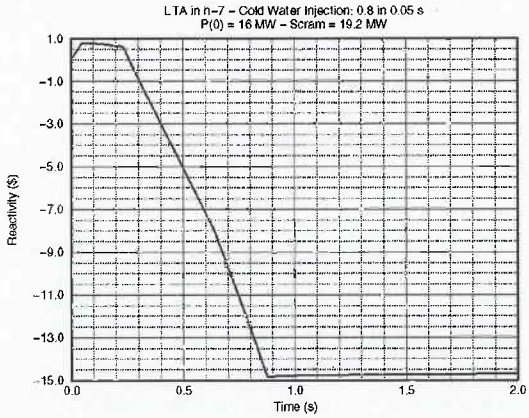

Figure 4.2.2.6.c Net Reactivity vs. Time for Cold Water Injection (0.8 $ Step) at 16 MW in HEU+LTA-h7 Core

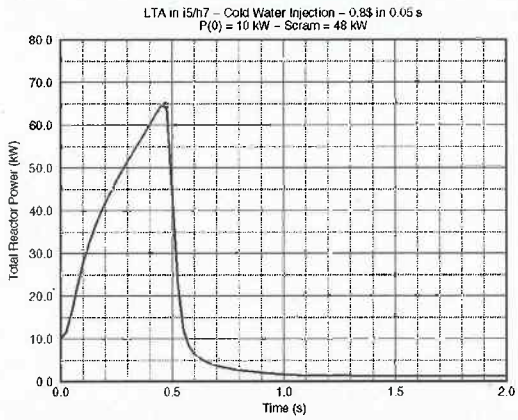

Figure 4.2.2.7.a Power vs. Time for Cold Water Injection (0.8 $ Step) at 10 kW in HEU+LTA-i5-h7 Core

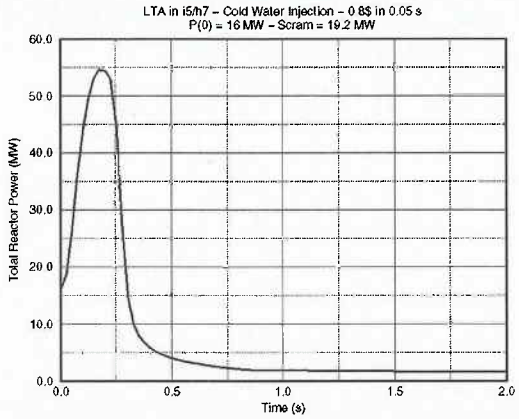

Figure 4.2.2.8.a Power vs. Time for Cold Water Injection (0.8 $ Step) at 16 MW in HEU+LTA-i5-h7 Core

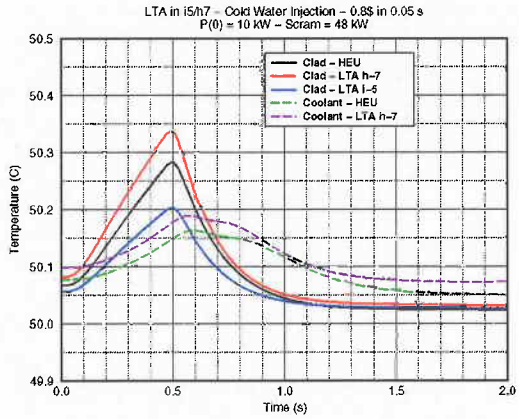

Figure 4.2.2.7.b Temperature vs. Time for Cold Water Injection (0.8 $ Step) at 10 kW in HEU+LTA-i5-h7 Core

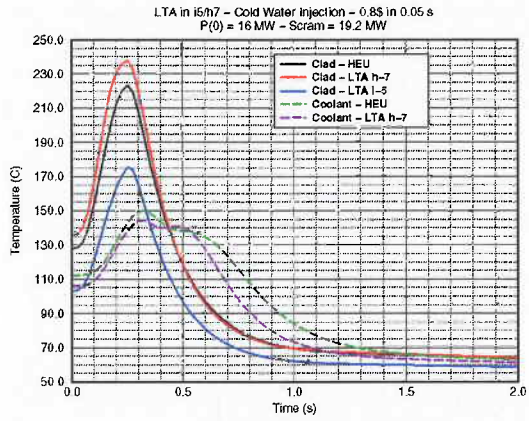

Figure 4.2.2.8.b Temperature vs. Time for Cold Water Injection (0.8 $ Step) at 16 MW in HEU+LTA-i5-h7 Core

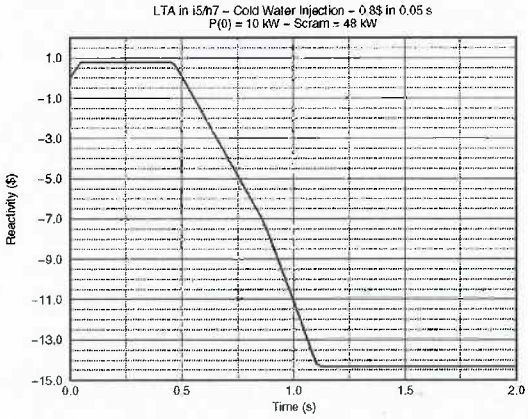

Figure 4.2.2.7.c Net Reactivity vs. Time for Cold Water Injection (0.8 $ Step) at 10 kW in HEU+LTA-i5-h7 Core

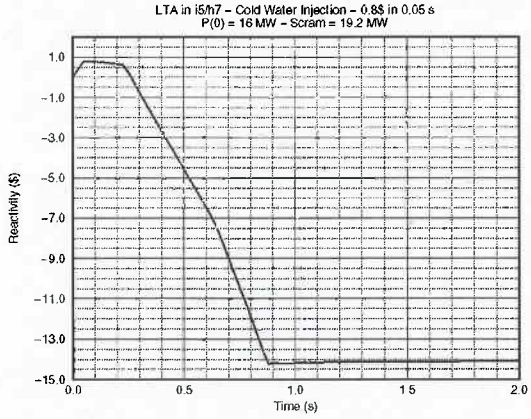

Figure 4.2.2.8.c Net Reactivity vs. Time for Cold Water Injection (0.8 $ Step) at 16 MW in HEU+LTA-i5-h7 Core

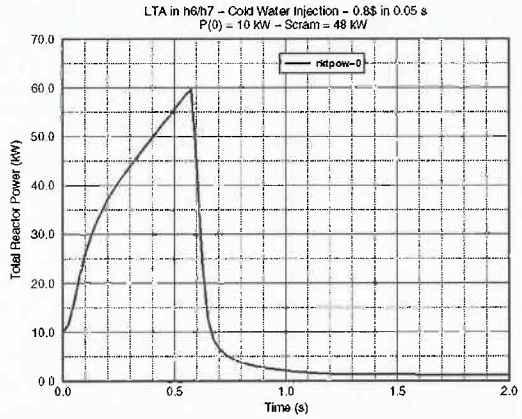

Figure 4.2.2.9.a Power vs. Time for Cold Water Injection (0.8 $ Step) at 10 kW in HEU+LTA-h6-h7 Core

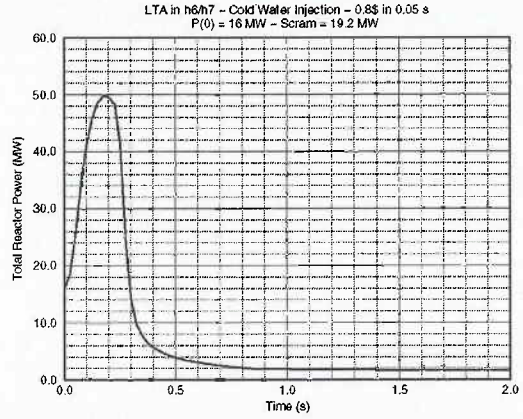

Figure 4.2.2.10.a Power vs. Time for Cold Water Injection (0.8 $ Step) at 16 MW in HEU+LTA-h6-h7 Core

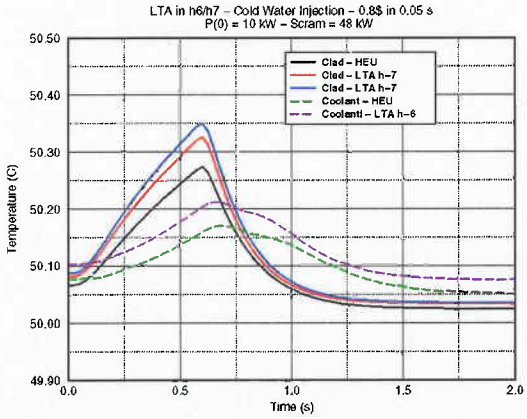

Figure 4.2.2.9.b Temperature vs. Time for Cold Water Injection (0.8 $ Step) at 10 kW in HEU+LTA-h6-h7 Core

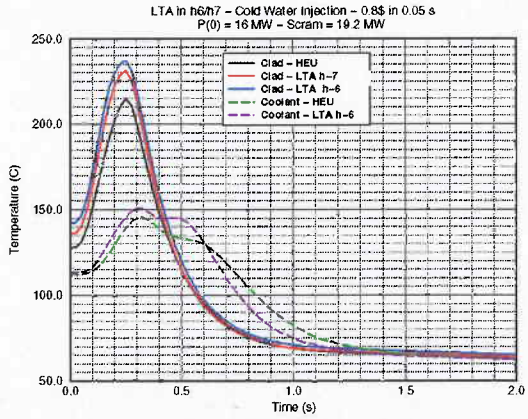

Figure 4.2.2.10.b Temperature vs. Time for Cold Water Injection (0.8 $ Step) at 16 MW in HEU+LTA-h6-h7 Core

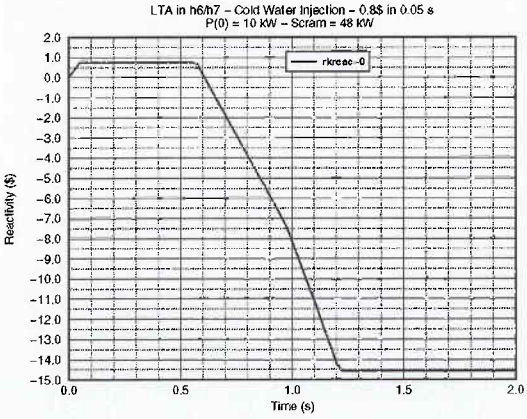

Figure 4.2.2.9.c Net Reactivity vs. Time for Cold Water Injection (0.8 $ Step) at 10 kW in HEU+LTA-h6-h7 Core

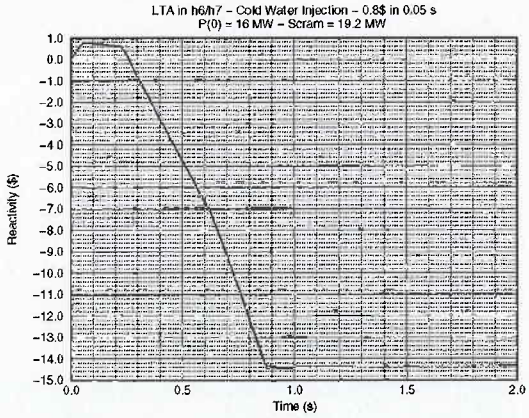

Figure 4.2.2.10.c Net Reactivity vs. Time for Cold Water Injection (0.8 $ Step) at 16 MW in HEU+LTA-h6-h7 Core

4.3. Fast Reactivity Insertion

4.3.1. Boundary Conditions

This transient is initiated by reactivity insertion at a rate of 4 $/s up to a total of 1.5 $ total. A mechanistic basis for this transient is break of the maximum worth control rod and drop of the broken part.

4.3.2. Results

The results computed using RELAP5 for this transient starting from low power in the HEU core are shown in Figure 4.3.2.1. The rapid reactivity addition causes the power to rise, crossing the 48 kW scram setting at about 0.3 s. The control rods start moving into the core 0.2 s later, at which time the power peaks at about 3.4 MW. By 0.6 s the power is less than the initial value and continues decreasing. The peak cladding temperature is 57.5°C at peak power and has decreased to less than the initial value after 1.5 s; no clad damage would be expected based on these temperature changes. Figure 4.3.2.1.c shows the reactivity addition over 0.38 s and essentially no reactivity feedbacks until scram, which is -15 $ in 0.64 s. With the reactor subcritical and temperatures decreasing there is no need to consider a longer time span than that shown here for this case.

The results computed for this transient starting from high power in the HEU core are shown in Figure 4.3.2.2. The rapid reactivity addition causes the power to rise, crossing the 19.2 MW scram setting in about 0.08 s. The control rods start moving into the core 0.2 s later, at which time the power had peaked at about 71 MW. By 0.35 s the power is less than the initial value and continues decreasing. The peak cladding temperature is 235°C at its peak and has decreased to less than the initial value after 0.55 s; no clad damage would be expected based on these temperature changes. Figure 4.3.2.2.c shows the reactivity addition over 0.38 s, a small decrease in reactivity as temperature rises, and insertion of the scram reactivity, which is -15 $ in 0.64 s. With the reactor subcritical and temperatures decreasing there is no need to consider a longer time span than that shown here for this case.

The results are shown in Figures 4.3.2.3 and 4.3.2.4 for the core with LTA in i-5, in Figures 4.3.2.5 and 4.3.2.6 for the core with LTA in h-7, in Figures 4.3.2.7 and 4.3.2.8 for the core with LTA in i-5 and h-7, and in Figures 4.3.2.9 and 4.3.2.10 for the core with LTA in h-6 and h-7. The following discussion will only highlight differences among these cores.

For the cases starting at low power there is essentially no difference in peak power or its timing. The peak clad temperature is less that 60°C for all cores; the peak clad temperature is slightly higher or lower reflecting the differences in the peak power density at steady state.

For the cases starting at high power, the peak power varies from 70 to 76 MW at 0.28 s. The peak clad temperature in the HEU FA having the peak power density ranges from 230-232°C. The peak clad temperature in the LEU LTA ranges from 183-253°C which reflects the differences in steady-state temperatures which are due to the differences in peak power density.

For the core with LTA in h-6 and h-7, the peak clad temperatures in the LTAs are higher than the peak in the HEU FA. No clad damage would be expected based on these temperature changes.

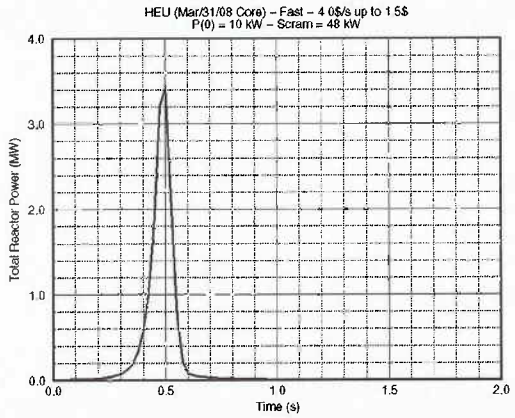

Figure 4.3.2.1.a Power vs. Time for 4 $/s Ramp at 10 kW in HEU Core

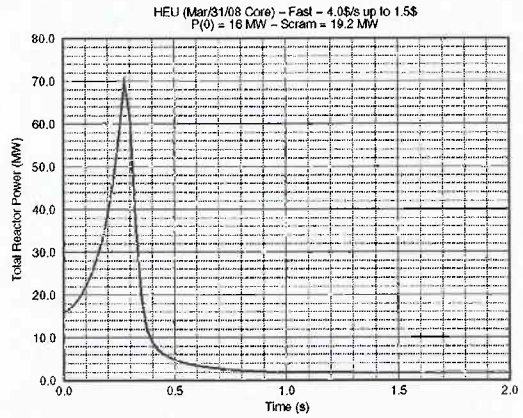

Figure 4.3.2.2.a Power vs. Time for 4 $/s Ramp at 16 MW in HEU Core

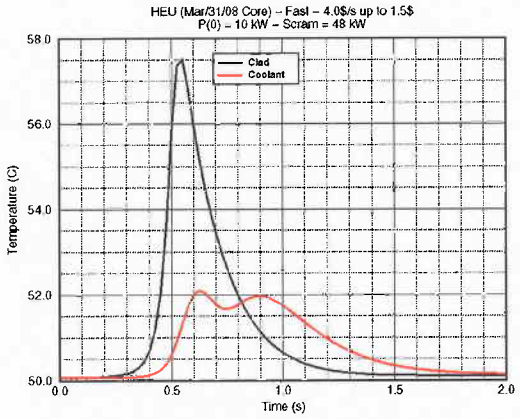

Figure 4.3.2.1.b Temperature vs. Time for 4 $/s Ramp at 10 kW in HEU Core

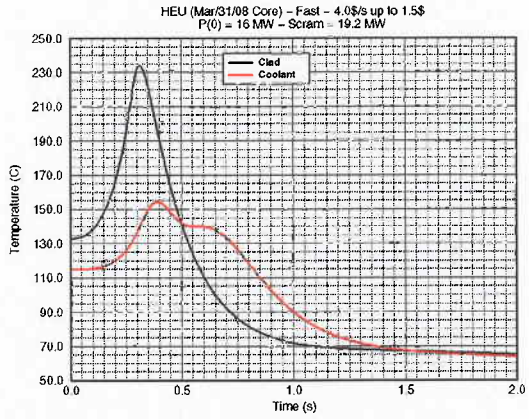

Figure 4.3.2.2.b Temperature vs. Time for 4 $/s Ramp at 16 MW in HEU Core

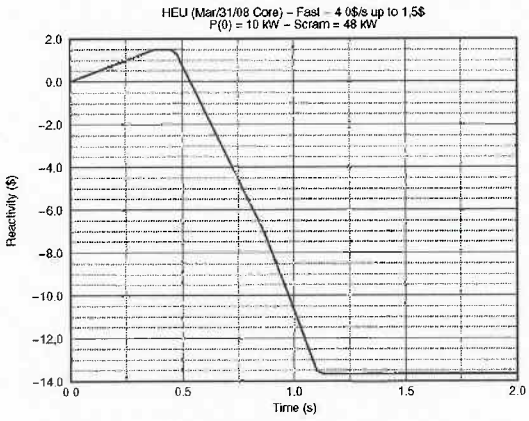

Figure 4.3.2.1.c Net Reactivity vs. Time for 4 $/s Ramp at 10 kW in HEU Core

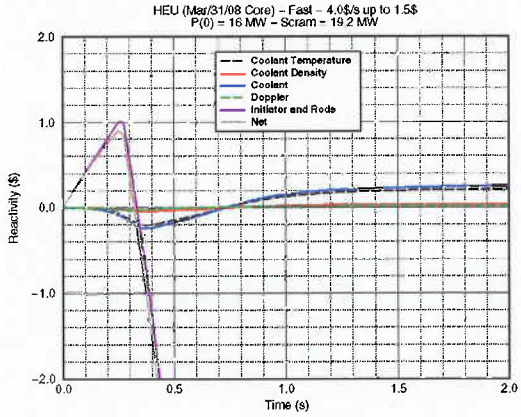

Figure 4.3.2.2.c Reactivity Components vs. Time for 4 $/s Ramp at 16 MW in HEU Core

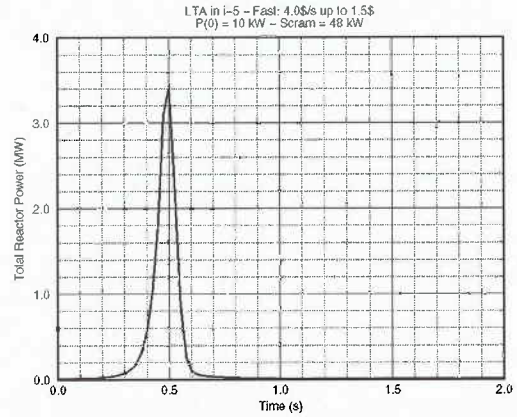

Figure 4.3.2.3.a Power vs. Time for 4 $/s Ramp at 10 kW in HEU+LTA-i5 Core

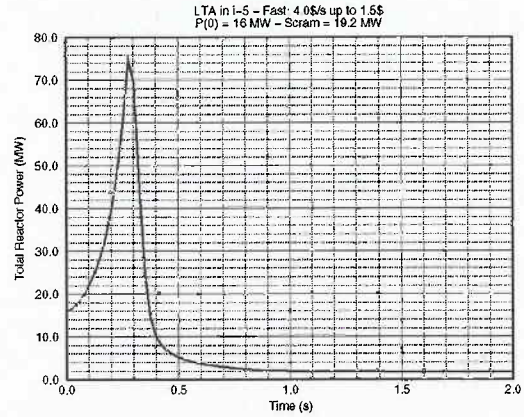

Figure 4.3.2.4.a Power vs. Time for 4 $/s Ramp at 16 MW in HEU+LTA-i5 Core

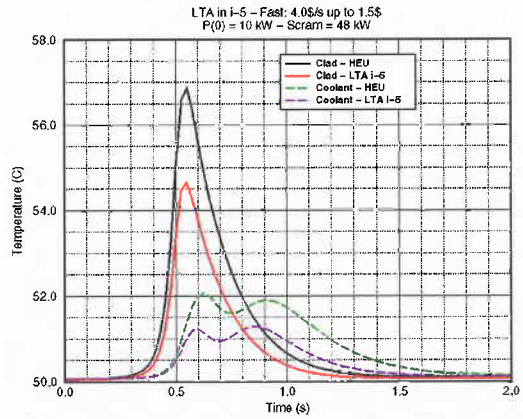

Figure 4.3.2.3.b Temperature vs. Time for 4 $/s Ramp at 10 kW in HEU+LTA-i5 Core

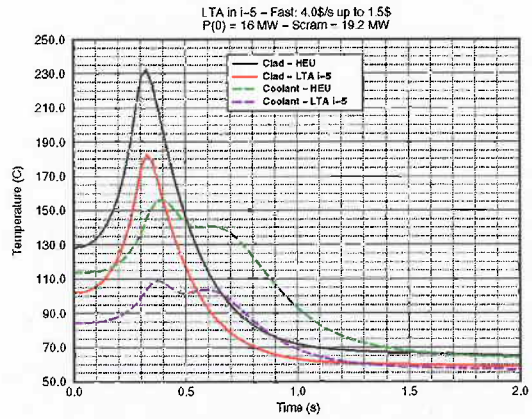

Figure 4.3.2.4.b Temperature vs. Time for 4 $/s Ramp at 16 MW in HEU+LTA-i5 Core

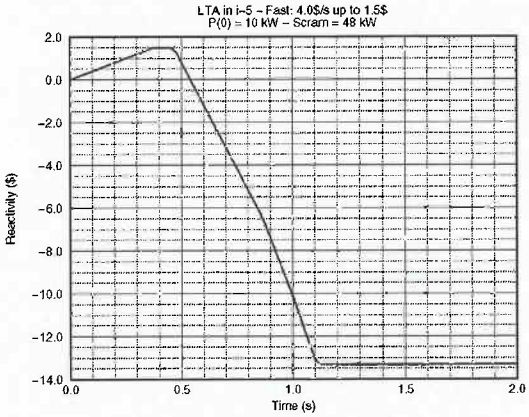

Figure 4.3.2.3.c Net Reactivity vs. Time for 4 $/s Ramp at 10 kW in HEU+LTA-i5 Core

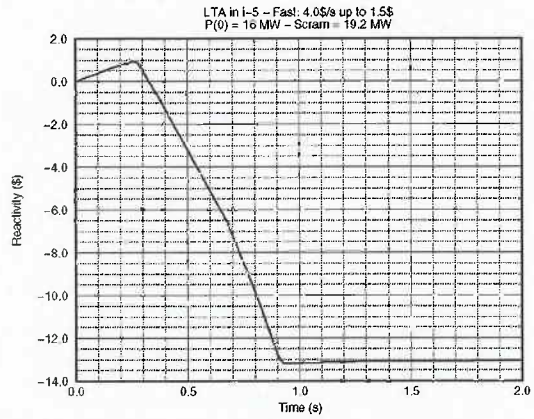

Figure 4.3.2.4.c Net Reactivity vs. Time for 4 $/s Ramp at 16 MW in HEU+LTA-i5 Core

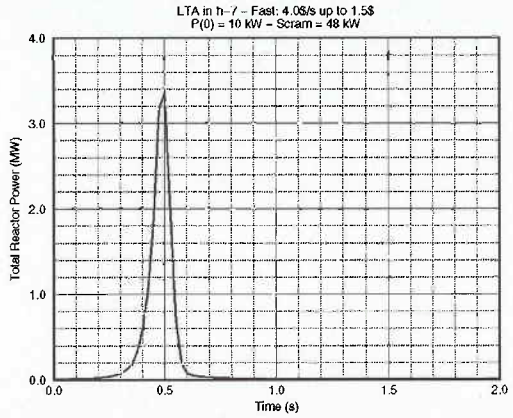

Figure 4.3.2.5.a Power vs. Time for 4 $/s Ramp at 10 kW in HEU+LTA-h7 Core

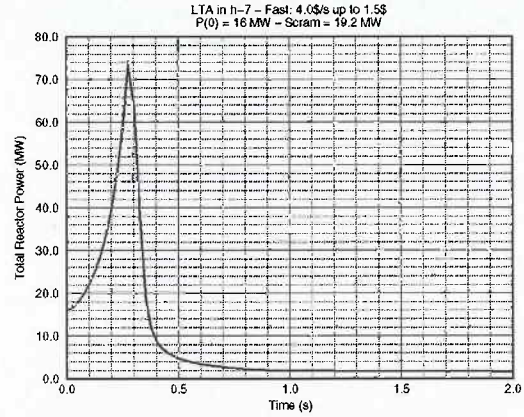

Figure 4.3.2.6.a Power vs. Time for 4 $/s Ramp at 16 MW in HEU+LTA-h7 Core

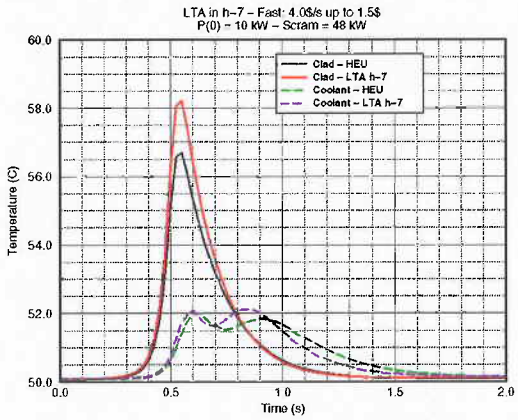

Figure 4.3.2.5.b Temperature vs. Time for 4 $/s Ramp at 10 kW in HEU+LTA-h7 Core

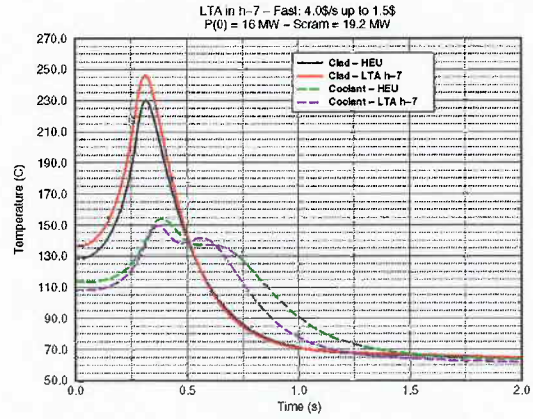

Figure 4.3.2.6.b Temperature vs. Time for 4 $/s Ramp at 16 MW in HEU+LTA-h7 Core

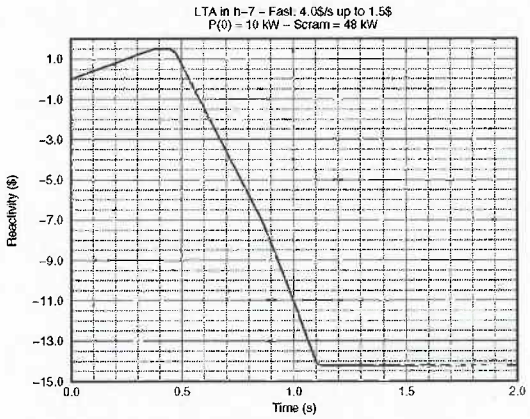

Figure 4.3.2.5.c Net Reactivity vs. Time for 4 $/s Ramp at 10 kW in HEU+LTA-h7 Core

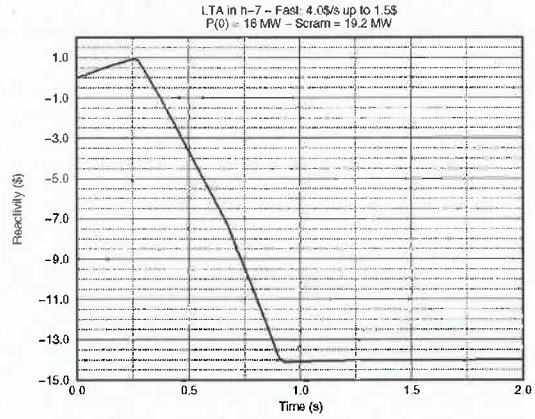

Figure 4.3.2.6.c Net Reactivity vs. Time for 4 $/s Ramp at 16 MW in HEU+LTA-h7 Core

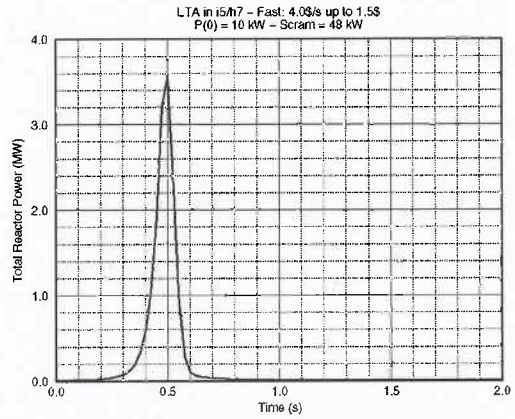

Figure 4.3.2.7.a Power vs. Time for 4 $/s Ramp at 10 kW in HEU+LTA-i5-h7 Core

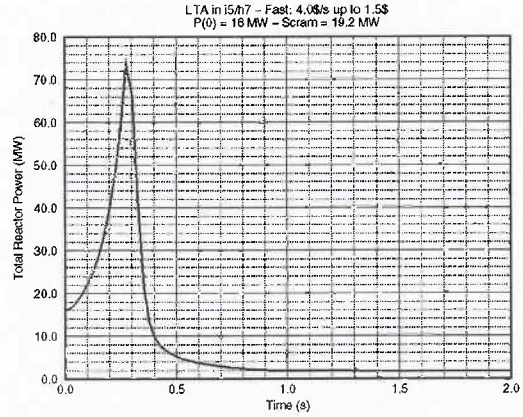

Figure 4.3.2.8.a Power vs. Time for 4 $/s Ramp at 16 MW in HEU+LTA-i5-h7 Core

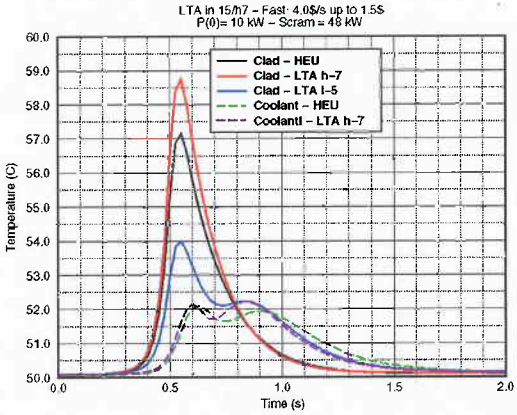

Figure 4.3.2.7.b Temperature vs. Time for 4 $/s Ramp at 10 kW in HEU+LTA-i5-h7 Core

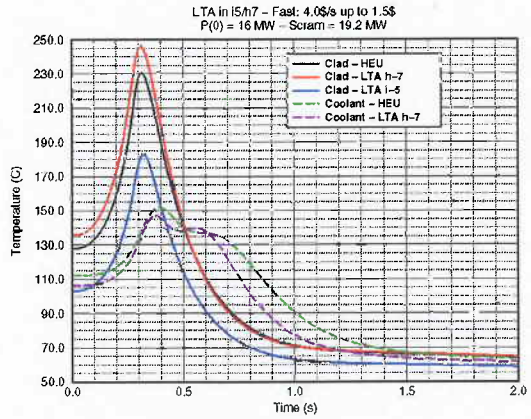

Figure 4.3.2.8.b Temperature vs. Time for 4 $/s Ramp at 16 MW in HEU+LTA-i5-h7 Core

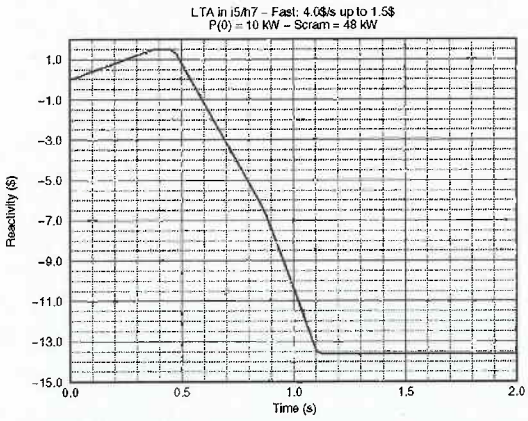

Figure 4.3.2.7.c Net Reactivity vs. Time for 4 $/s Ramp at 10 kW in HEU+LTA-i5-h7 Core

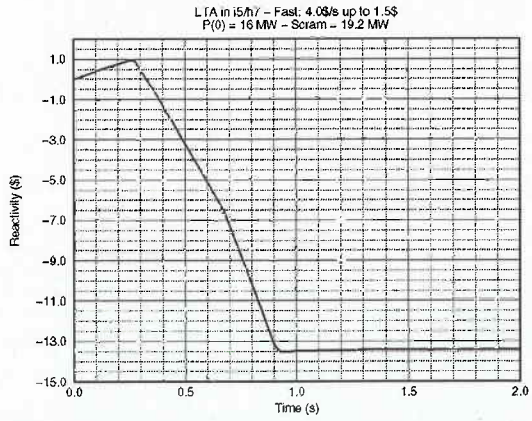

Figure 4.3.2.8.c Net Reactivity vs. Time for 4 $/s Ramp at 16 MW in HEU+LTA-i5-h7 Core

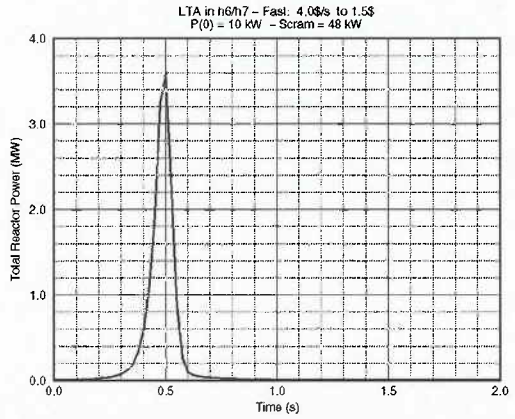

Figure 4.3.2.9.a Power vs. Time for 4 $/s Ramp at 10 kW in HEU+LTA-h6-h7 Core

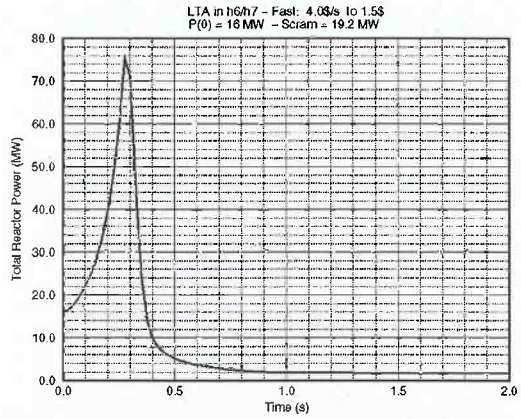

Figure 4.3.2.10.a Power vs. Time for 4 $/s Ramp at 16 MW in HEU+LTA-h6-h7 Core

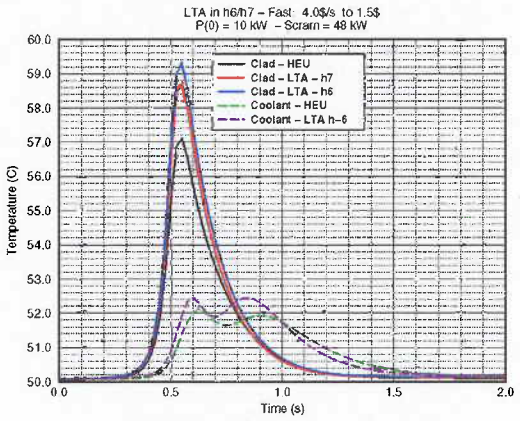

Figure 4.3.2.9.b Temperature vs. Time for 4 $/s Ramp at 10 kW in HEU+LTA-h6-h7 Core

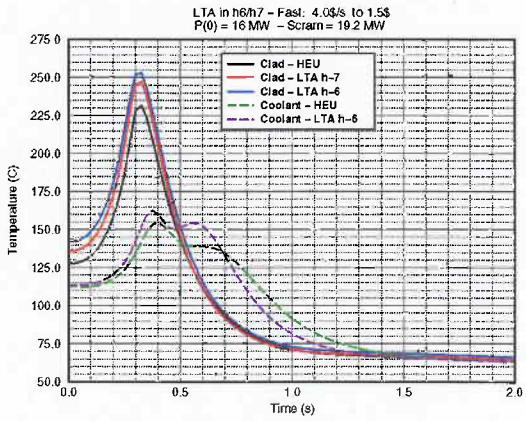

Figure 4.3.2.10.b Temperature vs. Time for 4 $/s Ramp at 16 MW in HEU+LTA-h6-h7 Core

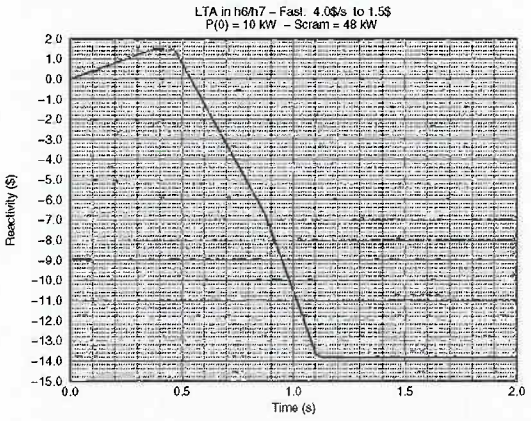

Figure 4.3.2.9.c Net Reactivity vs. Time for 4 $/s Ramp at 10 kW in HEU+LTA-h6-h7 Core

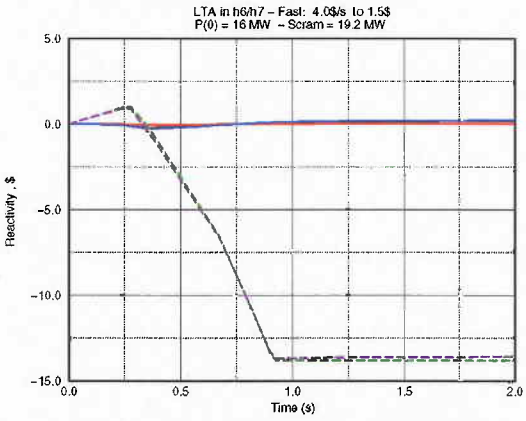

Figure 4.3.2.10.c Net Reactivity vs. Time for 4 $/s Ramp at 16 MW in HEU+LTA-h6-h7 Core

4.4. Slow Reactivity Insertion

4.4.1. Boundary Conditions

This transient is initiated by reactivity insertion at a rate of 0.04 $/s up to a total of 0.4 $ total. A mechanistic basis for this transient is uncontrolled withdrawal of the Power Automatic Rod (PAR) from its nominal mid-core axial position.

4.4.2. Results

The results computed using RELAP5 for this transient starting from low power in the HEU core are shown in Figure 4.4.2.1. The slow reactivity addition causes the power to rise, crossing the 48 kW scram setting at about 13 s. The control rods start moving into the core 0.2 s later, at which time the power peaks at about 50 kW. By 13.5 s the power is less than the initial value and continues decreasing. The peak cladding temperature is 50.3°C at peak power and has decreased to less than the initial value after 14 s; no clad damage would be expected based on these temperature changes. Figure 4.4.2.1.c shows the reactivity addition over 10 s and essentially no reactivity feedbacks until scram, which is -15 $ in 0.64 s. With the reactor subcritical and temperatures decreasing there is no need to consider a longer time span than that shown here for this case.

The results computed for this transient starting from high power in the HEU core are shown in Figure 4.4.2.2. The slow reactivity addition causes the power to rise, crossing the 19.2 MW scram setting in 4.2 s. The control rods start moving into the core 0.2 s later, at which time the power had peaked at 19.4 MW. By 4.5 s the power is less than the initial value and continues decreasing. The peak cladding temperature is 147°C at its peak and has decreased to less than the initial value after 4.6 s; no clad damage would be expected based on these temperature changes. Figure 4.4.2.2.c shows the reactivity addition over 0.44 s until insertion of the scram reactivity, which is -15 $ in 0.64 s. With the reactor subcritical and temperatures decreasing there is no need to consider a longer time span than that shown here for this case.

The results are shown in Figures 4.4.2.3 and 4.4.2.4 for the core with LTA in i-5, in Figures 4.4.2.5 and 4.4.2.6 for the core with LTA in h-7, in Figures 4.4.2.7 and 4.4.2.8 for the core with LTA in i-5 and h-7, and in Figures 4.4.2.9 and 4.4.2.10 for the core with LTA in h-6 and h-7. The following discussion will only highlight differences among these cores.

For the cases starting at low power there is essentially no difference in peak power or its timing. The peak clad temperature is less that 50.4°C for all cores; the peak clad temperature is slightly higher or lower reflecting the differences in the peak power density at steady state.

For the cases starting at high power there is essentially no difference in peak power or its timing. The peak clad temperature in the HEU FA having the peak power density ranges from 141-147°C. The peak clad temperature in the LEU LTA ranges from 112-158°C which reflects the differences in steady-state temperatures which are due to the differences in peak power density.

For the core with LTA in h-6 and h-7, the peak clad temperatures in the LTAs are higher than the peak in the HEU FA. No clad damage would be expected based on these temperature changes.

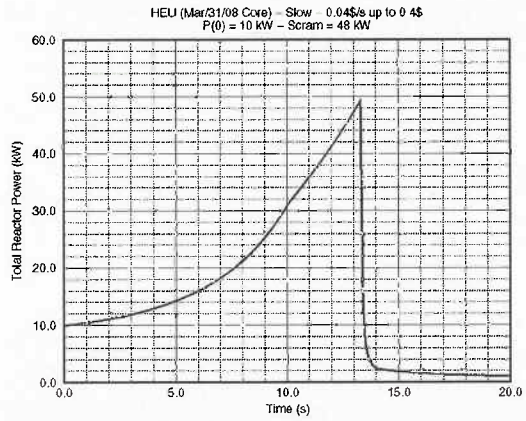

Figure 4.4.2.1.a Power vs. Time for 0.04 $/s Ramp at 10 kW in HEU Core

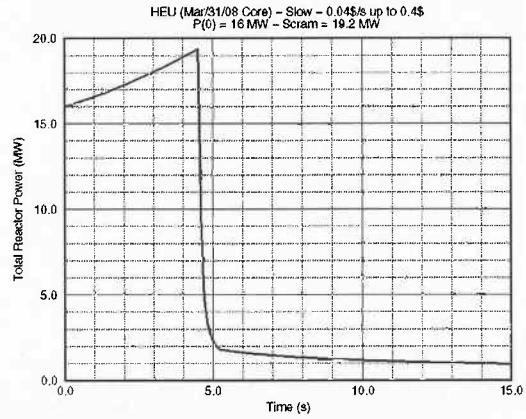

Figure 4.4.2.2.a Power vs. Time for 0.04 $/s Ramp at 16 MW in HEU Core

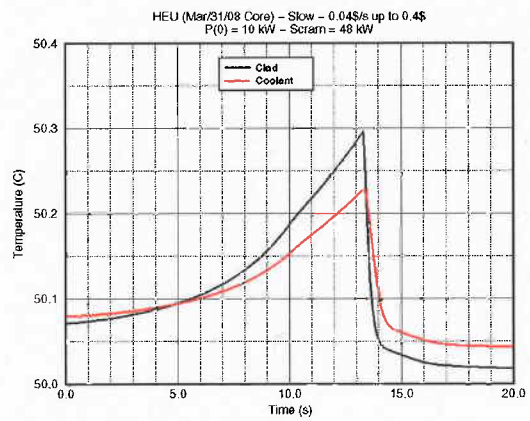

Figure 4.4.2.1.b Temperature vs. Time for 0.04 $/s Ramp at 10 kW in HEU Core

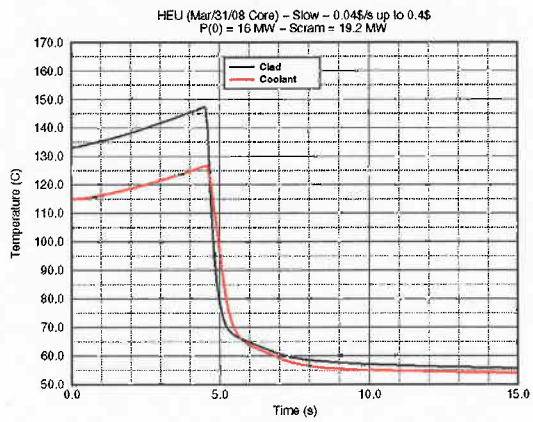

Figure 4.4.2.2.b Temperature vs. Time for 0.04 $/s Ramp at 16 MW in HEU Core

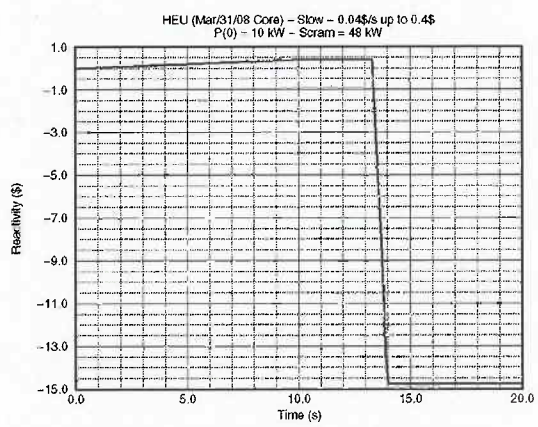

Figure 4.4.2.1.c Net Reactivity vs. Time for 0.04 $/s Ramp at 10 kW in HEU Core

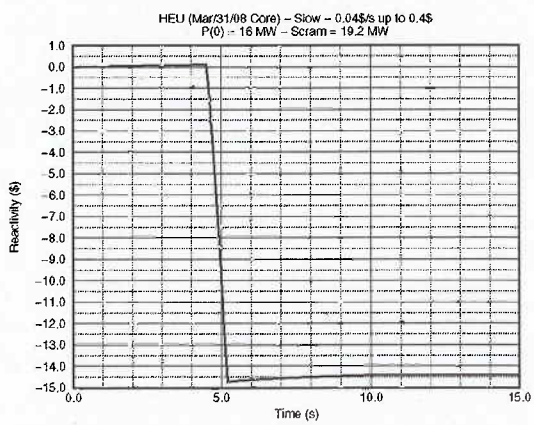

Figure 4.4.2.2.c Net Reactivity vs. Time for 0.04 $/s Ramp at 16 MW in HEU Core

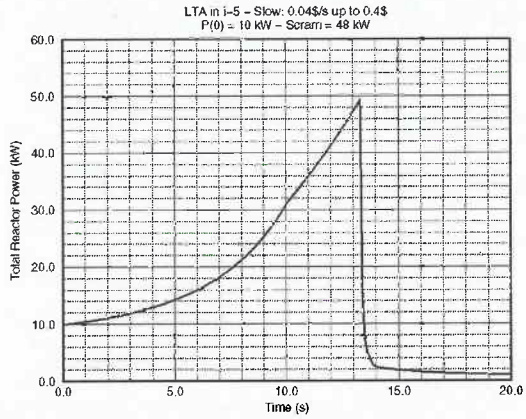

Figure 4.4.2.3.a Power vs. Time for 0.04 $/s Ramp at 10 kW in HEU+LTA-i5 Core

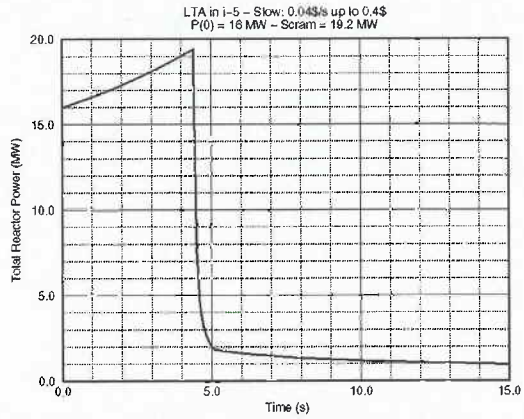

Figure 4.4.2.4.a Power vs. Time for 0.04 $/s Ramp at 16 MW in HEU+LTA-i5 Core

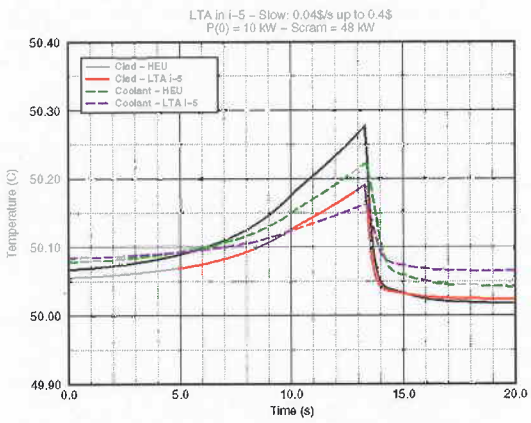

Figure 4.4.2.3.b Temperature vs. Time for 0.04 $/s Ramp at 10 kW in HEU+LTA-i5 Core

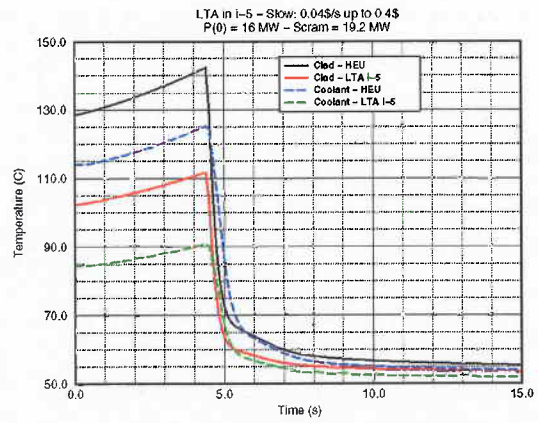

Figure 4.4.2.4.b Temperature vs. Time for 0.04 $/s Ramp at 16 MW in HEU+LTA-i5 Core

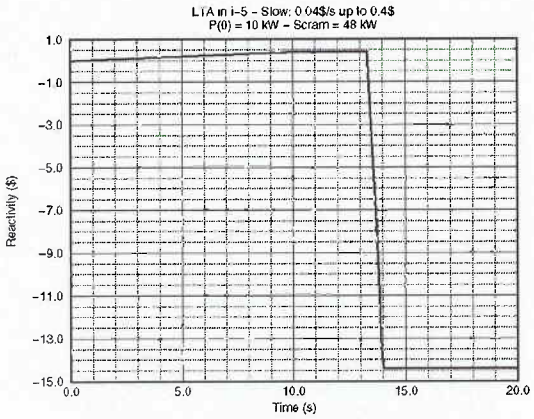

Figure 4.4.2.3.c Net Reactivity vs. Time for 0.04 $/s Ramp at 10 kW in HEU+LTA-i5 Core

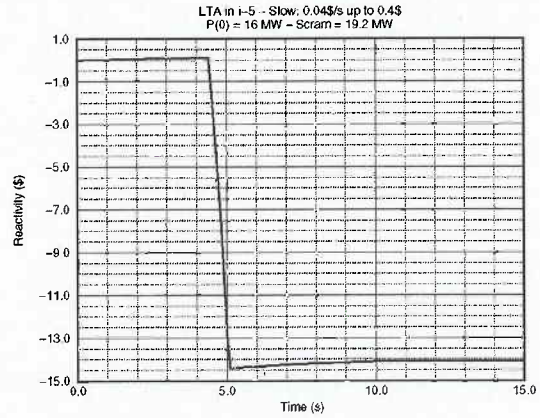

Figure 4.4.2.4.c Net Reactivity vs. Time for 0.04 $/s Ramp at 16 MW in HEU+LTA-i5 Core

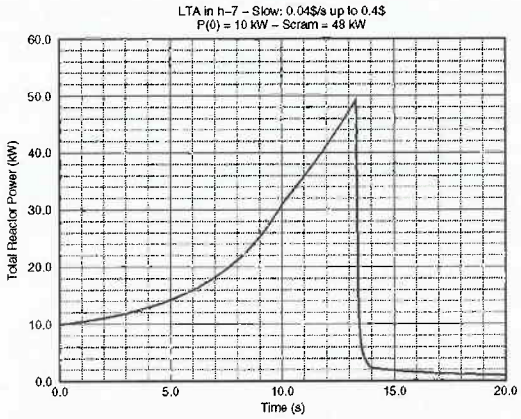

Figure 4.4.2.5.a Power vs. Time for 0.04 $/s Ramp at 10 kW in HEU+LTA-h7 Core

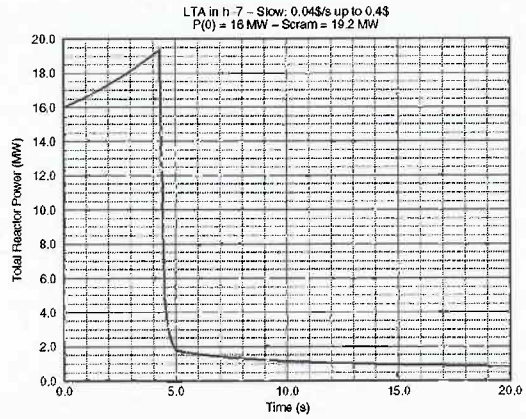

Figure 4.4.2.6.a Power vs. Time for 0.04 $/s Ramp at 16 MW in HEU+LTA-h7 Core

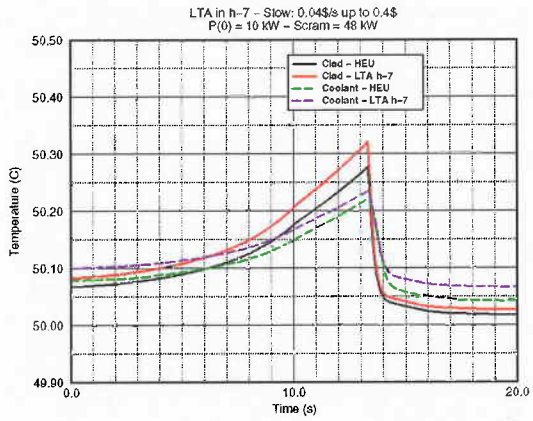

Figure 4.4.2.5.b Temperature vs. Time for 0.04 $/s Ramp at 10 kW in HEU+LTA-h7 Core

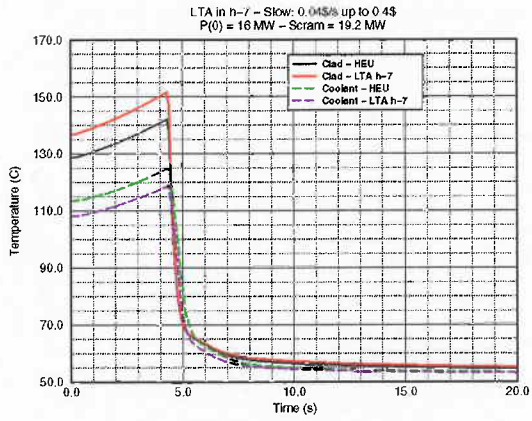

Figure 4.4.2.6.b Temperature vs. Time for 0.04 $/s Ramp at 16 MW in HEU+LTA-h7 Core

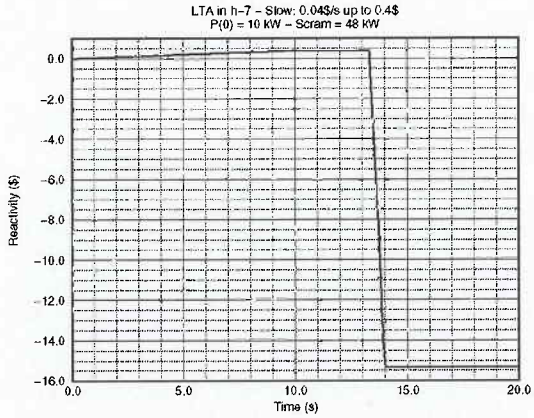

Figure 4.4.2.5.c Net Reactivity vs. Time for 0.04 $/s Ramp at 10 kW in HEU+LTA-h7 Core

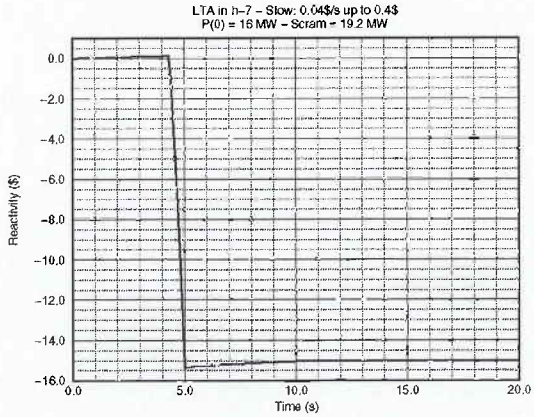

Figure 4.4.2.6.c Net Reactivity vs. Time for 0.04 $/s Ramp at 16 MW in HEU+LTA-h7 Core

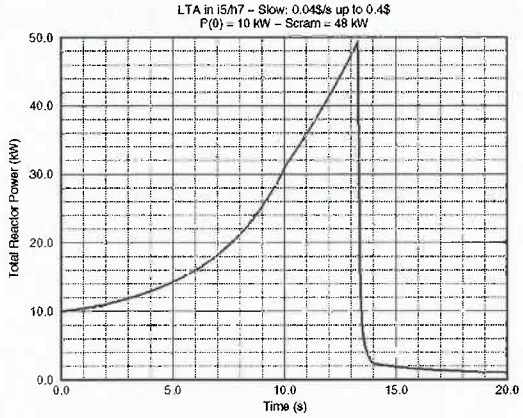

Figure 4.4.2.7.a Power vs. Time for 0.04 $/s Ramp at 10 kW in HEU+LTA-i5-h7 Core

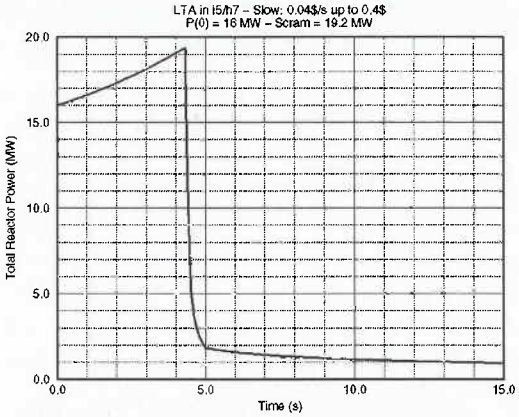

Figure 4.4.2.8.a Powervs. Time for 0.04 $/s Ramp at 16 MW in HEU+LTA-i5-h7 Core

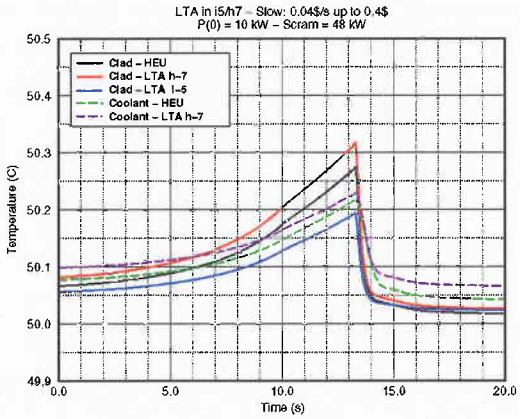

Figure 4.4.2.7.b Temperature vs. Time for 0.04 $/s Ramp at 10 kW in HEU+LTA-i5-h7 Core

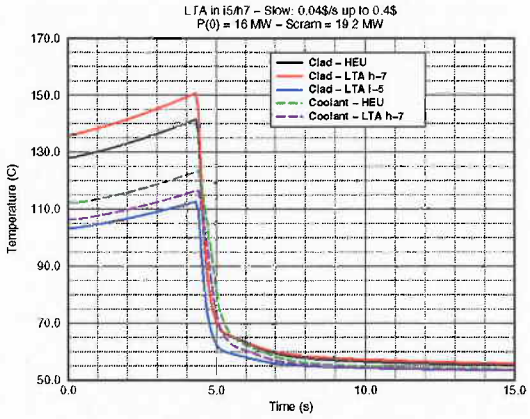

Figure 4.4.2.8.b Temperature vs. Time for 0.04 $/s Ramp at 16 MW in HEU+LTA-i5-h7 Core

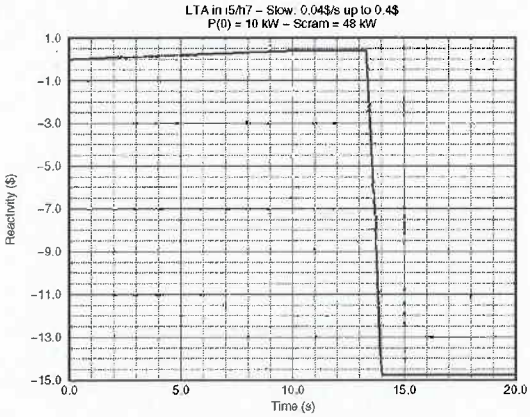

Figure 4.4.2.7.c Net Reactivity vs. Time for 0.04 $/s Ramp at 10 kW in HEU+LTA-i5-h7 Core

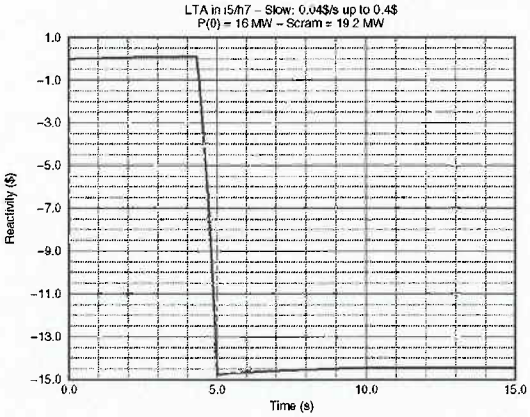

Figure 4.4.2.8.c Net Reactivity vs. Time for 0.04 $/s Ramp at 16 MW in HEU+LTA-i5-h7 Core

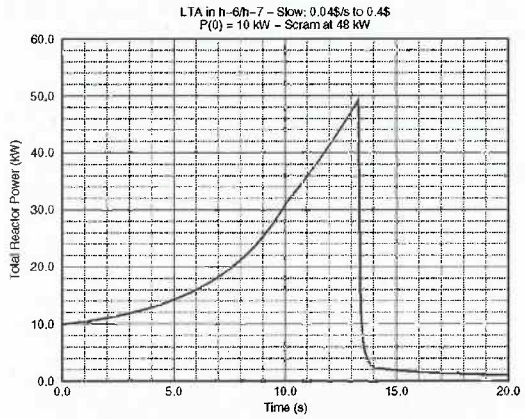

Figure 4.4.2.9.a Power vs. Time for 0.04 $/s Ramp at 10 kW in HEU+LTA-h6-h7 Core

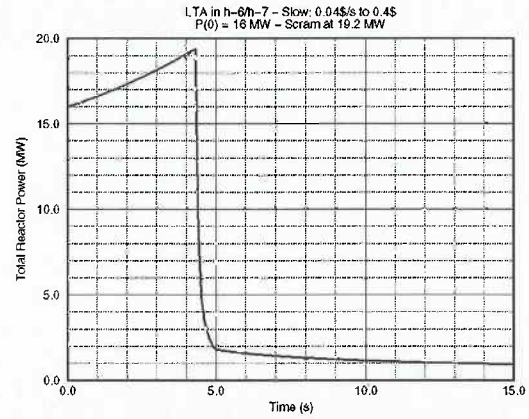

Figure 4.4.2.10.a Power vs. Time for 0.04 $/s Ramp at 16 MW in HEU+LTA-h6-h7 Core

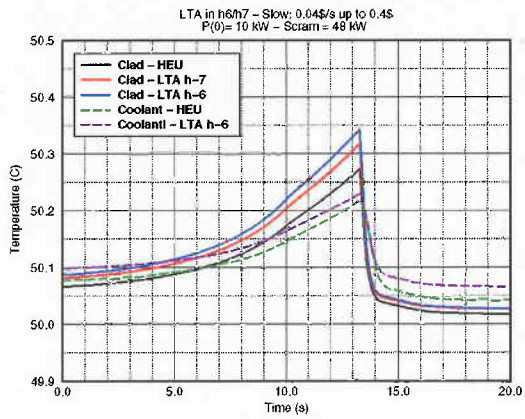

Figure 4.4.2.9.b Temperature vs. Time for 0.04 $/s Ramp at 10 kW in HEU+LTA-h6-h7 Core

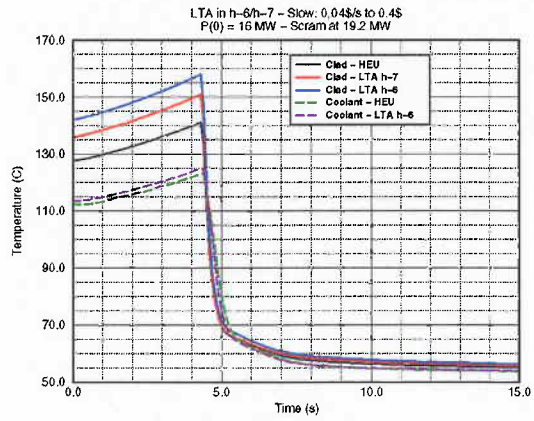

Figure 4.4.2.10.b Temperature vs. Time for 0.04 $/s Ramp at 16 MW in HEU+LTA-h6-h7 Core

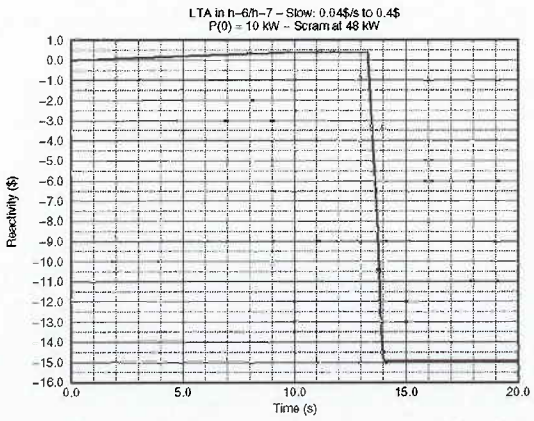

Figure 4.4.2.9.c Net Reactivity vs. Time for 0.04 $/s Ramp at 10 kW in HEU+LTA-h6-h7 Core

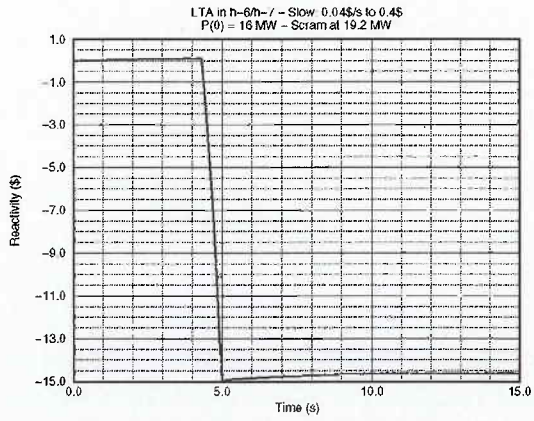

Figure 4.4.2.10.c Net Reactivity vs. Time for 0.04 $/s Ramp at 16 MW in HEU+LTA-h6-h7 Core

4.5. Transients Summary

For the three reactivity transients starting at low power the peak temperature is less than 60°C in all core configurations. There is no challenge to the clad.

For the three reactivity transients starting at high power, the peak clad temperatures are summarized in Table 4.5.1. The power and temperature reach the highest values in the fast insertion (i.e., Sec. 4.3), next highest in the cold water injection (i.e., Sec. 4.2), and the lowest in the slow insertion (i.e., Sec. 4.4). Within each of these transients, the highest power and temperature were obtained for the cores with two LTAs and the peak temperatures are in the LTAs rather than in the HEU portion of the core. Do keep in mind that (1) the spread in peak clad temperatures across the 5 core configurations was only 21°C for the fast insertion and (2) the peak clad temperature is not high enough in any of these cases to cause significant clad damage.

Table 4.5.1 Maximum Clad Temperature in Transients

	T-clad-max [°C]	
Transient	HEU	LEU LTA
Cold Water Inject (0.8$ Step)	226	237
Fast Ramp (4 $/s)	235	253
Slow Ramp (0.04 $/s)	147	158

5. Conclusions

Calculations have been performed to analyze the behavior of adding two LEU LTAs to the MARIA reactor. There is little change to the overall neutronics parameters. At steady state without hot channel factors the peak clad temperature in the LEU LTA is 144.7°C versus 136.3°C in the all-HEU core; when hot channel factors are included the peak clad temperature is 186.5°C in the LEU LTA versus 170.8°C in the all-HEU core. Based on having ONBR greater than 1.2 with hot channel factors, the power in the LEU LTA will need to remain less than 1.5 MW (note that the maximum calculated value for the power in the LTA was 1.44 MW) versus 1.9 MW in an HEU FA. Peak clad temperature during postulated reactivity transients is 253°C in the LEU LTAs versus 235°C in the HEU; these temperatures are sufficiently low and for sufficiently short duration that no clad damage is expected for these transients.

6. References and Computer Files

1. "MARIA Reactor Operations", Chapter 2 in *Annual Report 2007*, http://www.iea.cyf.gov.pl/pdf/ar_2007/reactor_maria/Chp_2_Maria%20Reactor.pdf, Institute of Atomic Energy, Swierk, POLAND (2007).
2. "Reactor Construction and Characteristics", Chapter 5 in *MARIA Safety Analysis Report*, Institute of Atomic Energy, Swierk, POLAND (2003).
3. "CERCA Design", email from W. Mieleszczenko (IAE) to N. Hanan (ANL) (January 22, 2008).
4. J. F. Briesmeister et al., "MCNP – A General Monte Carlo N-Particle Transport Code, Version 4C", LA-13709-M, Los Alamos National Laboratory, Los Alamos, New Mexico (April 2000).
5. N. A. Hanan, A. P. Olson, R. B. Pond, and J. E. Matos, "A Monte Carlo Burnup Code Linking MCNP and REBUS", *Proceedings of the 21st International Meeting on Reduced Enrichment for Research and Test Reactors*, Sao Paulo, Brazil (October 18-23, 1998).
6. "RELAP5/MOD3 Code Manual", NUREG/CR-5535 (or INEL-95/0174), Idaho National Engineering Laboratory, Idaho Falls, Idaho (June 1995).
7. P. L. Garner and N. A. Hanan, "Investigation of Approximations in Thermal-Hydraulic Modeling of Core Conversions", submitted for presentation at presented at *2007 International RERTR Meeting* (Prague, Czech Republic), http://www.rertr.anl.gov/RERTR29/, Argonne National Laboratory, Argonne, Illinois, (September 23 – 28, 2007).
8. "STAR-CD Methodology", "STAR-CD User Guide", and other related reports, version 4.04, CD adapco Group, Melville, New York (2007).
9. "CERCA Design", email from W. Mieleszczenko (IAE) to N. Hanan (ANL) (February 1, 2008).
10. Roger Ricque and Roger Siboul, "Ebullition Locale De L'eau En Convection Forcee", Report VEA-R-3984, Centre d'Etudes Nucleaires de Grenoble, France (May 1970). *[This is the reference for Forster-Greif ONB correlation.]*
11. E. E. Feldman, "Hot Channel Factors Treatment", Appendix IV in Arne P. Olson and M. Kalimullah, *A Users Guide to the PLTEMP/ANL V3.5 Code*, Argonne National Laboratory, Argonne, Illinois (May 30, 2008).

Computer files associated with RELAP5 analyses for this work are stored on node *sol15* under directories *~hanan/iea06/mar3108/threl/core/final* where *core* is one of *heu*, *ltai5*, *ltah7*, *ltai5h7*, or *ltah6h7*.

Nuclear Engineering Division
Argonne National Laboratory
9700 South Cass Avenue, Bldg. 208
Argonne, IL 60439-4842

www.anl.gov

Argonne National Laboratory is a U.S. Department of Energy laboratory managed by UChicago Argonne, LLC